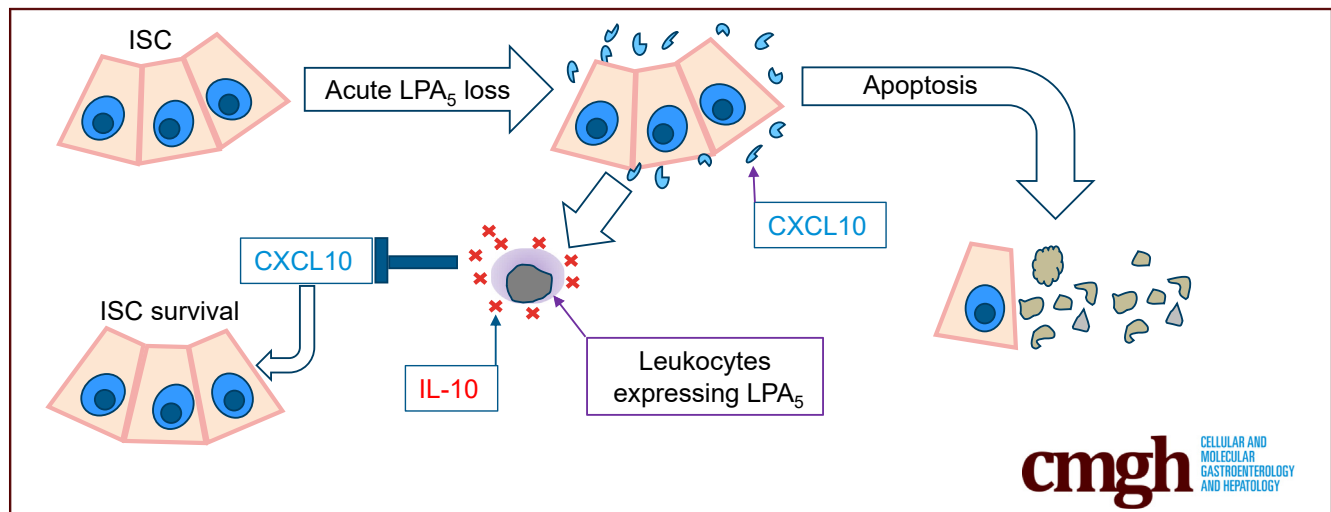


ORIGINAL RESEARCH

Survival of Stem Cells and Progenitors in the Intestine Is Regulated by LPA₅-Dependent SignalingZhongxing Liang,¹ Peijian He,¹ Yiran Han,¹ and C. Chris Yun^{1,2,3}¹Division of Digestive Diseases, Department of Medicine, Emory University School of Medicine, Atlanta, Georgia;²Gastroenterology Research, Atlanta Veterans Administration Medical Center, Decatur, Georgia; and ³Winship Cancer Institute, Emory University School of Medicine, Atlanta, Georgia

SUMMARY

Lysophosphatidic acid, a bioactive phospholipid, mediates multiple cellular effects. Using a conditional knockout mouse, we show that lysophosphatidic acid receptor 5 is necessary for the survival of stem cells and progenitors in the intestine.

BACKGROUND & AIMS: Regeneration of the epithelium by stem cells in the intestine is supported by intrinsic and extrinsic factors. Lysophosphatidic acid (LPA), a bioactive lipid mediator, regulates many cellular functions, including cell proliferation, survival, and cytokine secretion. Here, we identify LPA₅ receptor as a potent regulator of the survival of stem cells and transit-amplifying cells in the intestine.

METHODS: We have used genetic mouse models of conditional deletion of *Lpar5*, *Lpar5^{f/f};Rosa-Cre^{ERT}* (*Lpar5^{KO}*), and intestinal epithelial cell-specific *Lpar5^{f/f};AhCre* (*Lpar5^{IECKO}*) mice. Mice were treated with tamoxifen or β -naphthoflavone to delete *Lpar5* expression. Enteroids derived from these mice were used to determine the effect of *Lpar5* loss on the apoptosis and proliferation of crypt epithelial cells.

RESULTS: Conditional loss of *Lpar5* induced ablation of the intestinal mucosa, which increased morbidity of *Lpar5^{KO}* mice. Epithelial regeneration was compromised with increased apoptosis and decreased proliferation of crypt epithelial cells

by *Lpar5* loss. Interestingly, intestinal epithelial cell-specific *Lpar5* loss did not cause similar phenotypic defects in vivo. *Lpar5* loss reduced intestinal stem cell marker gene expression and reduced lineage tracing from *Lgr5⁺* ISCs. *Lpar5* loss induced CXCL10 expression which exerts cytotoxic effects on intestinal stem cells and progenitors in the intestinal crypts. By co-culturing *Lpar5^{KO}* enteroids with wild-type or *Lpar5^{KO}* splenocytes, we demonstrated that lymphocytes protect the intestinal crypts via a LPA₅-dependent suppression of CXCL10.

CONCLUSIONS: LPA₅ is essential for the regeneration of intestinal epithelium. Our findings reveal a new finding that LPA₅ regulates survival of stem cells and transit-amplifying cells in the intestine. (*Cell Mol Gastroenterol Hepatol* 2022;14:129–150; <https://doi.org/10.1016/j.jcmgh.2022.03.012>)

Keywords: Gastrointestinal; LPA; Epithelial Cell Survival.

The surface of the intestinal tract is lined with a monolayer of columnar epithelial cells that forms a physical and functional barrier separating the complex luminal milieu from the mucosal layer of the gut. The epithelium in the small intestine is organized into the villi and crypts. *Lgr5⁺* (leucine-rich repeat-containing G protein-coupled receptor 5) stem cells residing at the base of crypts give rise to highly proliferative transit-amplifying (TA) cells. Cellular differentiation occurs as cells migrate out of the crypt onto the flanks of the villi.¹ The entire

epithelium is renewed every 4–5 days. The stem cells are nourished by the microenvironment surrounding the crypts or stem cell niche that provide necessary repertoire of growth factors.² Recently, immune cells have emerged as key components of the stem cell niche.^{2,3} In particular, CD4⁺ T helper cells have been shown to be essential in preserving the integrity of *Lgr5*⁺ intestinal stem cells (ISCs).³

The CXC chemokines play a key role in inflammation. CXCL10 (previously called interferon gamma [IFN- γ]-inducible protein 10) was initially discovered as a chemokine induced by IFN- γ that recruits leukocytes, such as T cells, monocytes, and eosinophils.⁴ In the intestine, several types of cells, including monocytes,⁵ endothelial cells,⁶ and intestinal epithelial cell (IECs),^{7,8} express CXCL10. Elevated levels of CXCL10 were observed in murine models of acute graft-vs-host disease, suggesting its role in allogenic stem cell transplantation.⁹ Patients with active inflammatory bowel disease (IBD)¹⁰ or celiac disease⁸ have elevated CXCL10 levels. Blockade CXCL10 protects mice from acute colitis by impairing T helper-1 induction¹¹ and enhancing crypt cell survival,¹² demonstrating its therapeutic potential for IBD.

Lysophosphatidic acid (LPA) is a naturally occurring phospholipid that is a potent inducer of cell proliferation, and as such its effects on tumor cell growth are well established.¹³ The effects of LPA are mediated through 6 distinct LPA receptors (LPARs), termed LPA₁-LPA₆ (gene names *Lpar1*-*Lpar6*), which activate major cellular signaling pathways, including the Wnt, phosphoinositide 3-kinase (PI3K), and epidermal growth factor (EGF) pathways.¹³ The expression of LPAR in embryonic stem cells^{14,15} and neural stem cells,^{16,17} along with the effects of LPA on neural development¹⁸ and myeloid differentiation,¹⁹ has been reported. A recent study using mouse enteroids showed that LPA can be used instead of EGF to support enteroid growth.²⁰ These studies have prompted potential roles of LPA and its receptors on stem cells and progenitors. However, it remains paradoxical that none of the LPAR-deficient mice display abnormality that can be attributed to impaired survival or maintenance of stem cells.

Lpar5 is highly expressed in gastrointestinal (GI) tract and brain.^{14,21} A series of studies have shown the importance of LPA₅ in the homeostatic functions in the gut. We have shown that LPA₅ activates the brush border Na⁺/H⁺ exchanger 3, which regulates Na⁺ and fluid absorption in the intestine,^{22,23} and LPA₅ regulates the intestinal epithelial permeability that controls bacterial translocation in the gut.²⁴ Unlike other LPARs, LPA₅ can be activated by the dietary protein hydrolysate and peptone.²⁵ LPA₅ expression is also detected on sensory nerves in the enteric nerve system of mouse intestinal mucosa, where it is activated by mesenteric lymphatic fluid, suggesting its role as a nutrient sensor.²⁶

In the present study, we show that LPA₅ is essential for the maintenance of the intestinal epithelium. Inducible deletion of *Lpar5* in adult mice resulted in intestinal crypt ablation associated with increased apoptosis of IECs in the crypt compartment. We identified chemokine CXCL10 as a major factor demising ISCs and TA cells, and as such


neutralizing CXCL10 protected these cells. Unlike global loss of *Lpar5*, IEC-specific *Lpar5* loss, however, did not cause intestinal epithelial atrophy in vivo, suggesting that other nonepithelial cells must protect the ISCs and TA cells. Coculturing *Lpar5*-deficient enteroids with wild-type (WT) splenocytes, but not *Lpar5*-deficient splenocytes, protected crypt epithelial cells from apoptosis through interleukin (IL)-10-dependent regulation of CXCL10. Thus, LPA₅ maintains ISCs and promotes proliferation of progenitors, and defective LPA₅ function induces epithelial cell apoptosis in the crypt via induction of CXCL10.

Results

Inducible Deletion of *Lpar5* Increases Mortality in Mice With Defects in the Gut

To assess the role of LPA₅ in the intestine, we crossed *Lpar5*^{fl/fl} mice²³ with *Rosa26-Cre*^{ERT} mice, generating a mouse model of inducible *Lpar5* knockout, *Lpar5*^{fl/fl};*Rosa-Cre*^{ERT}. We administered tamoxifen (TAM) (40 mg/kg/d) for 5 days to adult *Lpar5*^{fl/fl};*Rosa-Cre*^{ERT} mice to delete *Lpar5*, which are referred to as *Lpar5*^{KO} hereafter. Surprisingly, *Lpar5*^{KO} showed a significant body weight loss with diarrhea (Figure 1A). *Lpar5*^{KO} mice were moribund or died by day 11. Necropsy revealed gross changes in the GI tract. The GI tract was pale and distended along its entire length filled with fluid and ingesta was present in the stomach (Figure 1B). Formed fecal pellets were not present in the colon of *Lpar5*^{KO} mice. Other organs in *Lpar5*^{KO} mice, including the liver, kidney, or heart, looked grossly normal, although it is possible that these organs have cellular changes that were not apparent by a visual examination. Histological examinations of *Lpar5*^{KO} mouse intestine revealed villus blunting associated with epithelial blobbing on the villi, immune cell infiltration, and crypt erosion in the small intestine compared with control mice (Figure 1C and D). The colon of *Lpar5*^{KO} mice displayed similar luminal damage and mild crypt hyperplasia (Figure 1C and D). The gross defects in *Lpar5*^{KO} mice were in striking contrast to the previous findings that constitutive knockout of *Lpar5* did not display a phenotype although blunted responses to neuropathic pain was observed in these mice.²⁷

Abbreviations used in this paper: β -NF, β -naphthoflavone; CC3, cleaved caspase 3; EGF, epidermal growth factor; ELISA, enzyme-linked immunosorbent assay; FBS, fetal bovine serum; GI, gastrointestinal; IBD, inflammatory bowel disease; IEC, intestinal epithelial cell; IFN- γ , interferon gamma; IL, interleukin; ISC, intestinal stem cell; Lgr5, leucine-rich repeat-containing G protein-coupled receptor 5; LPA, lysophosphatidic acid; LPAR, lysophosphatidic acid receptor; mRNA, messenger RNA; PBS, phosphate-buffered saline; PI3K, phosphoinositide 3-kinase; RT-PCR, reverse-transcription polymerase chain reaction; TA, transit amplifying; TAM, tamoxifen; tdT, tdTomato fluorescence protein; TNF- α , tumor necrosis factor α ; TUNEL, terminal deoxynucleotide transferase-mediated deoxyuridine triphosphate nick-end labeling; WT, wild-type.

 Most current article

© 2022 The Authors. Published by Elsevier Inc. on behalf of the AGA Institute. This is an open access article under the CC BY-NC-ND license (<http://creativecommons.org/licenses/by-nc-nd/4.0/>).

2352-345X

<https://doi.org/10.1016/j.jcmgh.2022.03.012>

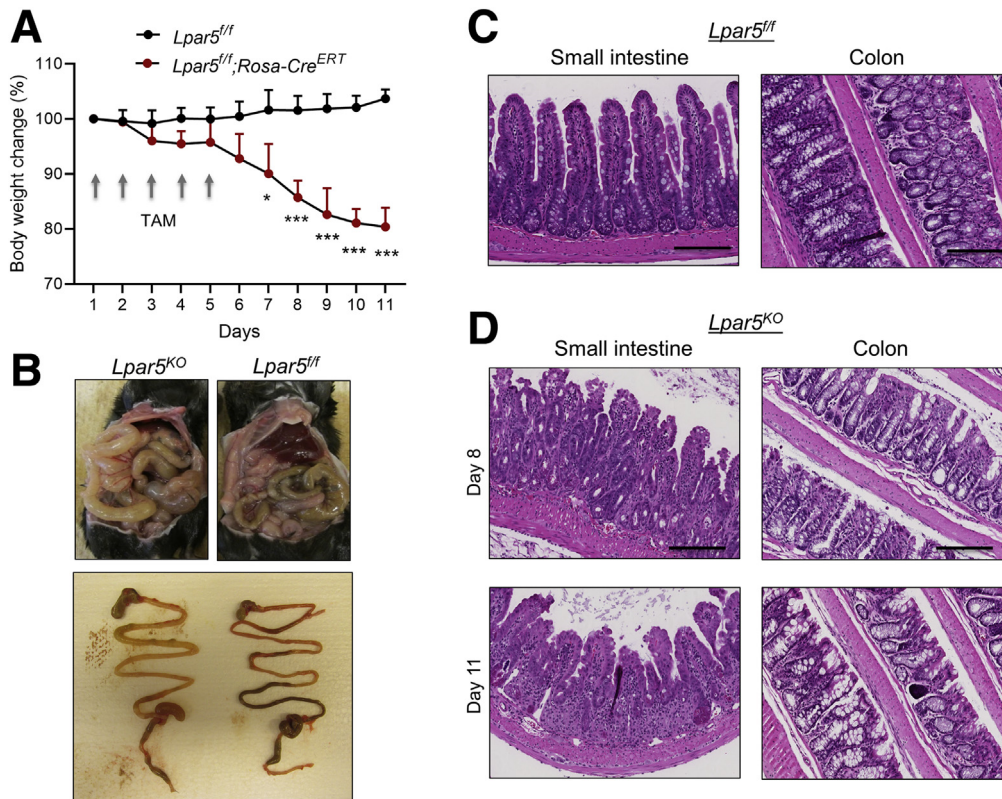


Figure 1. *Lpar5* loss induces inflammation in the intestine with epithelial damage. (A) *Lpar5^{ff}* and *Lpar5^{ff};RosaCre^{ERT}* mice were administered TAM (40 mg/kg/d) for 5 days and body weights were determined. Initial body weight of each group was set at 100%. $n = 3$. All data are presented as mean \pm SD. * $P < .05$, *** $P < .01$ compared with *Lpar5^{ff}* mice by 1-way analysis of variance with Tukey's multiple comparison test. Representative of 3 experiments. (B) The representative appearances of the abdomen of TAM-treated *Lpar5^{ff}* and *Lpar5^{KO}* mice on day 11 are shown. Bottom panel shows typical appearance of the gastrointestinal tract of *Lpar5^{KO}* and *Lpar5^{ff}* mice. (C) Hematoxylin and eosin–stained images of the small intestine and colon of *Lpar5^{ff}* mice. (D) Representative sections from the small intestine and colon of *Lpar5^{KO}* mice on day 8 and 11. Scale bar = 200 μ m.

Loss of *Lpar5* Causes Intestinal Crypt Cell Apoptosis

The mucosal ablation in *Lpar5^{KO}* mice may have been caused by premature loss of mature IECs at the villus tips or loss of crypt epithelial cells that compromises the renewal of the intestinal epithelium. In either case, we expected to observe increased epithelial cell death and hence we analyzed epithelial cell apoptosis in the small intestine of *Lpar5^{ff}* and *Lpar5^{KO}* mice by immunostaining for cleaved caspase 3 (CC3). We observed increased CC3 levels in the crypt compartments of *Lpar5^{KO}* small intestine, but there was no apparent CC3 labeling at the villi (Figure 2A), indicating that the initial effect of *Lpar5* loss is primarily on proliferating crypt epithelial cells. To determine the spatiotemporal relationship between *Lpar5* deletion and IEC death, *Lpar5^{ff};Rosa-Cre^{ERT}* mice were given high doses of TAM (100 mg/kg/d) for 2 days (day 0 and 1). TAM treatment rapidly decreased *Lpar5* expression in *Lpar5^{ff};Rosa-Cre^{ERT}* mice, reaching $\sim 90\%$ decrease within 14 hours (Figure 2B). The number of apoptotic cells gradually increased during the next several days (Figure 2C and D), demonstrating that crypt epithelial cell apoptosis is induced by *Lpar5* loss. At the same time, the number of proliferating

cells identified by EdU in the crypts decreased (Figure 2C and E). It has been shown previously that 100 mg/kg TAM can impair intestinal regeneration postirradiation, although the same concentration of TAM does not alter IEC proliferation or intestinal architecture under homeostatic conditions.²⁸ To ensure that the effects on high dose TAM in *Lpar5^{ff};Rosa-Cre^{ERT}* mice are specific to *Lpar5* loss, the effects of TAM on control *Lpar5^{ff}* mice were assessed. The rates of crypt epithelial cell proliferation and apoptosis in control mice were not altered by the TAM treatment, indicating that the effects are specific to *Lpar5* loss and not the cytotoxicity of TAM (Figure 2F).

The roles of epithelial LPA₅ in modulating Na⁺ transport and epithelial barrier functions have recently been demonstrated,^{22–24} but other types of cells, including endocrine cells,²⁵ lymphocytes,²⁹ macrophages,³⁰ and neurons,^{26,27} express LPA₅. Therefore, it is uncertain whether the observed crypt cell death in *Lpar5^{KO}* mice can be attributed to an autonomous effect of LPA₅ on IECs. To address this question, we cultured intestinal epithelial cell-derived enteroids.³¹ After the initial formation of enteroids, *Lpar5^{ff}* enteroids enlarged with the formation of crypt-like buds, and the growth of *Lpar5^{ff}* enteroids was not affected

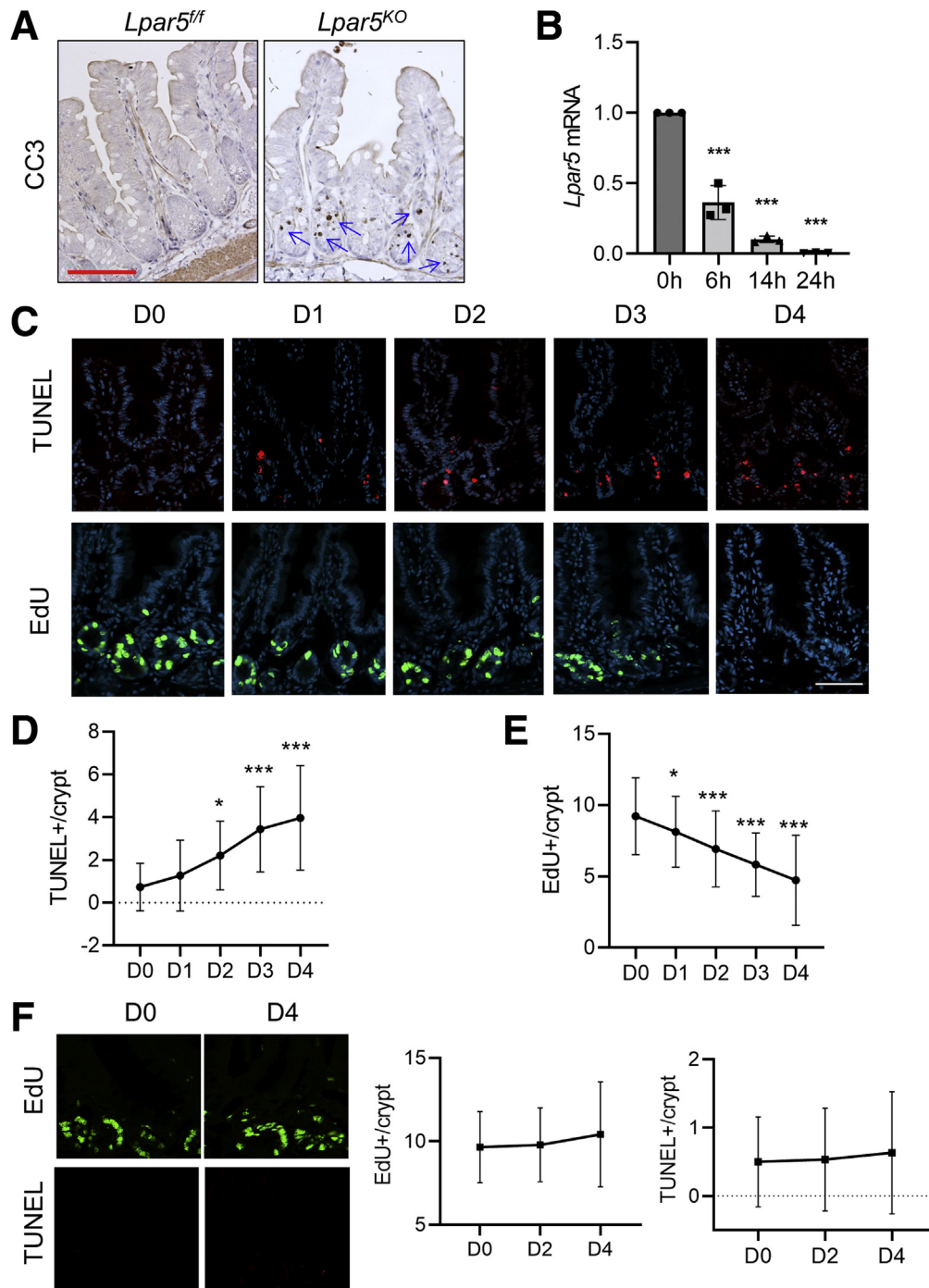


Figure 2. *Lpar5* loss induces in crypt epithelial cell apoptosis. (A) Representative images of immunohistochemical staining of CC3 in the jejunum of *Lpar5^{fl/fl}* and *Lpar5^{fl/fl};RosaCre^{ERT}* mice treated with 5× TAM. Apoptosis of IECs in the crypt compartment (blue arrows) of *Lpar5^{KO}* mice is indicated. Scale bar = 100 μ m. (B) *Lpar5* mRNA expression in *Lpar5^{fl/fl};RosaCre^{ERT}* mice treated with 100 mg/kg TAM was determined by quantitative RT-PCR. n = 3. ****P* < .001 compared with 0 hours. (C) Representative immunofluorescence images of apoptosis (TUNEL, red) and proliferation (EdU, green) of crypt epithelial cells in the jejunum of *Lpar5^{fl/fl}* and *Lpar5^{KO}* mice on each day of treatment are shown. Representative of 3 experiments. Scale bar = 50 μ m. (D) Quantification of TUNEL⁺ apoptosis per crypt from the jejunum. n = 30. (E) Quantification of EdU⁺ cells per crypt. n = 40. Representative of 3 independent experiments. All data are presented as mean \pm SD. **P* < .05, ****P* < .001 compared with day 0 (D0) by 1-way analysis of variance with Tukey's multiple comparison test. (F) Representative images of EdU and TUNEL staining in the jejunal sections of *Lpar5^{fl/fl}* mice treated with 100 mg/kg/d for 2 days are shown. Quantification of EdU⁺ and TUNEL⁺ cells per crypt on days 0, 2, and 4 are shown on the right. n = 90.

by the presence of 4OHT (Figure 3A, left panels). In contrast, we observed visible loss of epithelial integrity and an impairment of *Lpar5*^{ff}/*Rosa-Cre*^{ERT} enteroid growth by 4OHT treatment (Figure 3A [right panel] and B). Consistent with the observation in mouse intestinal crypts (Figure 2C), *Lpar5* loss induced IEC apoptosis while reducing proliferation in enteroids (Figure 3C). We confirmed the importance of LPA₅ on enteroid growth by treating WT enteroids with the LPA₅ inhibitor, TC LPA5 4, which blocked the growth of WT enteroids (Figure 3D). These results demonstrated that LPA₅ regulates IEC survival and proliferation.

IEC-Specific *Lpar5* Loss Does Not Cause Morbidity

Having observed the effect of *Lpar5* loss in enteroids, we questioned whether IEC-specific loss of *Lpar5* is sufficient for the mucosal ablation in the mouse intestine. To test this, we crossed *Lpar5*^{ff} mice with *AhCre* transgenic mice³² to generate a mouse strain with inducible IEC-specific *Lpar5* knockout, *Lpar5*^{ff}/*AhCre* or *Lpar5*^{IECKO}. Treating *Lpar5*^{ff}/*AhCre* with β -naphthoflavone (β -NF) (80 mg/kg/d) for 5 days reduced *Lpar5* expression by >90% in IECs. However, unlike *Lpar5*^{KO} mice, *Lpar5*^{IECKO} mice did not show any sign of illness up to 2 weeks post- β -NF treatment. We could not observe a notable change in the appearance of the intestinal crypts or villi of *Lpar5*^{IECKO} mice compared with control *Lpar5*^{ff} mouse (Figure 4A). Yet, terminal deoxynucleotide transferase-mediated deoxyuridine triphosphate nick-end labeling (TUNEL) staining revealed the occurrence of cell death in the intestinal crypts (Figure 4B), which was detected as early as 48 hours following the first β -NF treatment (Figure 4C). Nevertheless, the number of TUNEL⁺ cells per crypt in *Lpar5*^{IECKO} mice was about half of that in *Lpar5*^{KO} mice (Figure 4C vs Figure 2D), suggesting that the apoptotic signal must be greater in *Lpar5*^{KO} mice. Furthermore, the number of cells in the S-phase in *Lpar5*^{IECKO} intestinal crypts determined by EdU staining was reduced (Figure 4D and E). Although the effect of IEC-specific deletion of *Lpar5* in the intestinal epithelium was modest in vivo, β -NF-induced deletion of *Lpar5* completely impaired the growth of *Lpar5*^{IECKO} enteroids (Figure 4F) with significant effects on IEC proliferation and apoptosis (Figure 4G, left panels). β -NF alone had no effect on control *Lpar5*^{ff} enteroids (Figure 4G, right panels). These results corroborated that LPA₅ is important for the maintenance of intestinal crypts.

Lpar5 Loss Reduces Clonal Expansion of ISCs

Increased crypt cell apoptosis and the failure for enteroids to grow could have resulted from LPA₅-dependent loss of ISCs. To evaluate whether LPA₅ regulates ISCs, we labeled enteroids for OLFM4, an alternative stem cell marker expressed by *Lgr5*⁺ ISCs.³³ *Lpar5* deletion by β -NF in *Lpar5*^{IECKO} enteroids resulted in decreased abundance of OLFM4⁺ cells (Figure 5A). *Lpar5* deletion increased TUNEL⁺ staining in enteroids, but we could not locate the TUNEL⁺ staining in OLFM4⁺ cells with certainty (Figure 5A). However, this could have been due to the ill timing of the

disappearance of OLFM4, and DNA fragmentation detected by the TUNEL assay. The effect on OLFM4 expression was confirmed in vivo in which anti-OLFM4 immunoreactivity was significantly reduced in the intestine of both *Lpar5*^{IECKO} and *Lpar5*^{KO} mice compared with that of *Lpar5*^{ff} control mice (Figure 5B). Consistently, the transcript levels of several ISC markers, including *Lgr5*,³⁴ *Olfm4*,³³ *Smoc2*,³⁵ and *Ascl2*,³⁶ were decreased in *Lpar5*^{IECKO} mice (Figure 5C).

To ensure the effect of LPA₅ on ISCs, we crossed *Lpar5*^{ff} mice with *Lgr5-EGFP-ires-Cre*^{ERT2} mice, followed by crossing with *Rosa26-tdTomato* mice.³⁴ The resulting *Lpar5*^{ff}/*Lgr5-EGFP-IRES-Cre*^{ERT2}/*Rosa26-tdTomato* (*Lgr5* ^{Δ Lpar5}) mice and control *Lgr5-EGFP-ires-Cre*^{ERT2}/*Rosa26-tdTomato* (*Lgr5*^{Cont}) mice were treated with TAM for 5 days to facilitate simultaneous linear tracing and *Lpar5* ablation in *Lgr5*⁺ ISCs. *Lgr5*-driven lineage tracing labeled with tdTomato fluorescence protein (tdT) was detected in 37 \pm 2.7% of the small intestinal crypts of *Lgr5*^{Cont} mice (Figure 5D) due to the mosaic nature of expression in the *Lgr5-EGFP-ires-Cre*^{ERT2} knock-in mouse.³⁴ Consistent with the decreased OLFM4⁺ cells by *Lpar5* loss, we observed a significant decrease in tdT⁺ crypts (25.4 \pm 2.7%) in *Lgr5* ^{Δ Lpar5} mice (Figure 5D), demonstrating that ISC function is compromised in the absence of LPA₅. In addition, EGFP⁺ (enhanced green fluorescent protein-positive) *Lgr5* (*Lgr5*^{EGFP}) cell numbers were significantly reduced in *Lgr5* ^{Δ Lpar5} mice (4.26 \pm 1.04 in *Lgr5*^{Cont} vs 2.94 \pm 1.06 in *Lgr5* ^{Δ Lpar5}) (Figure 5E).

To determine whether *Lpar5* deletion affects the colony forming ability of ISCs in 3D cultures, *Lpar5*^{ff}/*Rosa-Cre*^{ERT} enteroids were dispersed and seeded in Matrigel in the presence or absence of 4OHT. Although we did not isolate *Lgr5*⁺ stem cells, we made an assumption that there are similar numbers of ISCs in both batches. Under this assumption, the number of enteroids initially formed was similar, but *Lpar5*^{KO} enteroids failed to grow and the most of the enteroids lost the integrity by day 3 (Figure 5F), confirming our earlier results that LPA₅ is necessary for the survival of enteroids. To assess the ability of ISCs to expand and form enteroids, *Lpar5*^{ff}/*Rosa-Cre*^{ERT} enteroids in Matrigel were treated with 4OHT or sunflower oil for 16 hours before passage. We observed a marked decrease in the number of enteroids initially formed by *Lpar5*^{KO} enteroids (Figure 5G), indicating that the clonal expansion efficiency of ISCs is diminished by *Lpar5* deletion.

Lpar5 Loss Increases CXCL10 Expression

LPA evokes various immune responses including chemotaxis, cytokine and chemokine secretion, and barrier regulation.³⁷ We postulated that *Lpar5* loss alters the expression of cytokines that induce epithelial cell apoptosis. We therefore screened a mouse cytokine array using conditioned media collected from *Lpar5*^{KO} and *Lpar5*^{ff} enteroids. We observed increased expression of CXCL10 in *Lpar5*^{KO} lysates (Figure 6A and Table 1). The expression levels of SDF-1 and C5a were decreased in *Lpar5*^{KO} enteroids, but the differences did not reach statistical significance. CXCL10 can trigger apoptosis of various cell types,³⁸⁻⁴⁰ while SDF-1⁴¹ and C5a⁴² are implicated in tissue

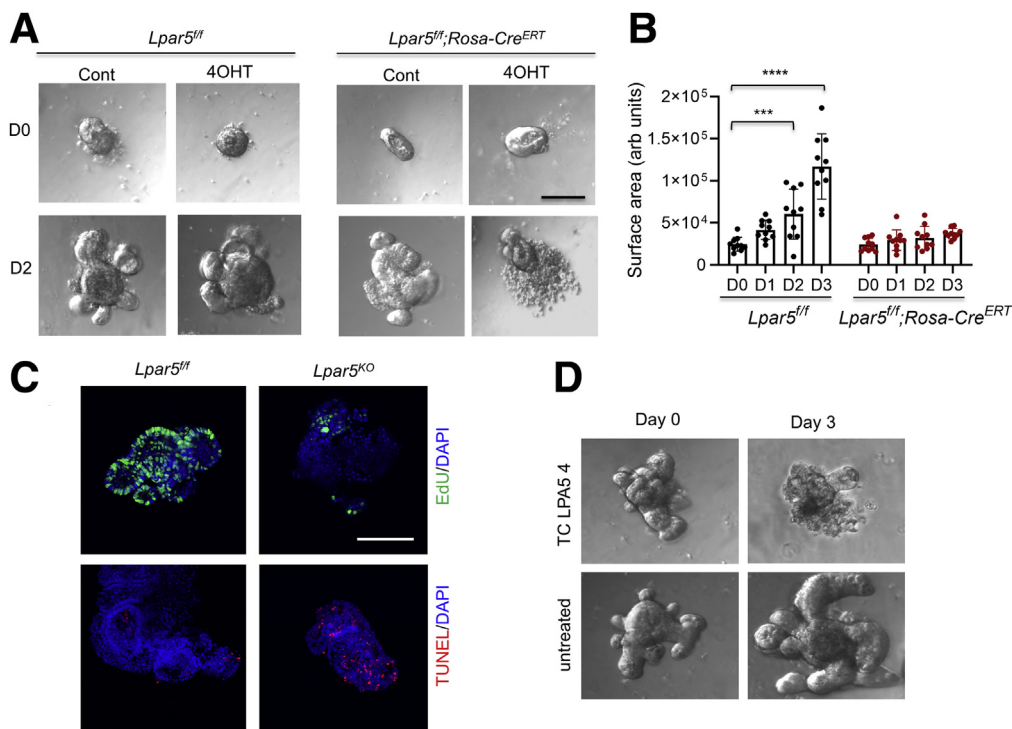


Figure 3. LPA₅ is necessary for the growth of enteroids. (A) *Lpar5^{fl/fl}* and *Lpar5^{fl/fl};RosaCre^{ERT}* mouse enteroids were treated with 1 μ M 4OHT or ethanol (Cont) on day 0 (D0). Representative images taken on day 2 (D2) are shown. Data are representative of >4 experiments. (B) The growth of enteroids in the presence of 4OHT was quantified by determining the surface area of enteroids using ImageJ 1.53k. All data are presented as mean \pm SD. *** P < .001, **** P < .0001 compared with D0 by 2-way analysis of variance with Tukey's multiple comparison test. n = 10. (C) Representative immunofluorescence images of EdU (green) and TUNEL (red) taken on D2 are shown. DAPI = blue. (D) WT enteroids were treated with TC LPA5 4 (5 μ M), an antagonist for LPA₅ for 3 days. Representative images from 3 experiments are shown.

repair and inflammation. Therefore, we postulated that CXCL10 is the probable candidate regulating IEC survival. The effect on CXCL10 expression was corroborated by increased *Cxcl10* messenger RNA (mRNA) levels in *Lpar5^{KO}* enteroids (Figure 6B). CXCL10 signals through its receptor CXCR3, which also binds CXCL9 and CXCL11.⁴³ However, the expression levels of CXCL9 and CXCL11 were not altered by *Lpar5* loss (Figure 6A and B). Given that the level of apoptosis was greater in *Lpar5^{KO}* mice along with severe mucosal damage compared with *Lpar5^{IECKO}* mice, we speculated CXCL10 levels to be different between *Lpar5^{KO}* and *Lpar5^{IECKO}* mice. Consistently, we found both mRNA (Figure 6C) and protein (Figure 6D) levels of CXCL10 to be elevated in *Lpar5^{KO}* mice compared with *Lpar5^{IECKO}* mice. CXCL10 was initially identified as an IFN- γ -inducible protein,⁴⁴ and because CXCL10 expression levels in *Lpar5^{KO}* mice were greater than in *Lpar5^{IECKO}* mice, we questioned whether IFN- γ levels were also elevated in *Lpar5^{KO}* mice. Indeed, IFN- γ expression in *Lpar5^{KO}* mice was significantly higher than *Lpar5^{IECKO}* mice (Figure 6E). Lymphocytes are a major producer of IFN- γ in the intestine,⁴⁵ and hence we assessed the presence of T cells in the intestinal mucosa by immunofluorescence staining for CD4. In keeping with the difference in IFN- γ levels, there were stepwise increases in CD4⁺ cell abundance from control mice to *Lpar5^{IECKO}* and to *Lpar5^{KO}* mice (Figure 6F and G), demonstrating the

correlation along the T cell-IFN- γ -CXCL10 axis in the absence of LPA₅.

CXCL10 Induces LPA₅-Dependent Epithelial Cell Apoptosis

To determine whether CXCL10 can induce IEC apoptosis, we treated enteroids with recombinant CXCL10. CXCL10 resulted in a concentration-dependent increase of TUNEL⁺ signals (Figure 7A). We next determined whether blockade of CXCL10 signaling by neutralizing anti-CXCL10 (α -CXCL10) antibody can prevent *Lpar5*-dependent cell death in mouse enteroids. As shown in Figure 7B, the integrity of the enteroids was preserved by α -CXCL10 antibody compared with IgG treated control animals. In addition, the size of enteroid with α -CXCL10 antibody increased (Figure 7C), indicating that the enteroid growth was resumed by neutralization of CXCL10. As expected, decreased levels of apoptosis (Figure 7D and E) and increased cell proliferation (Figure 7D and F) were observed in enteroids treated with α -CXCL10 antibody. To determine whether α -CXCL10 antibody protects stem cells, we determined OLFM4 expression in enteroids. As shown in Figure 7G and quantified in Figure 7H, α -CXCL10 antibody mitigated the loss of OLFM4⁺ cells by 4OHT. Consistent with the change in OLFM4 expression, the colony-forming

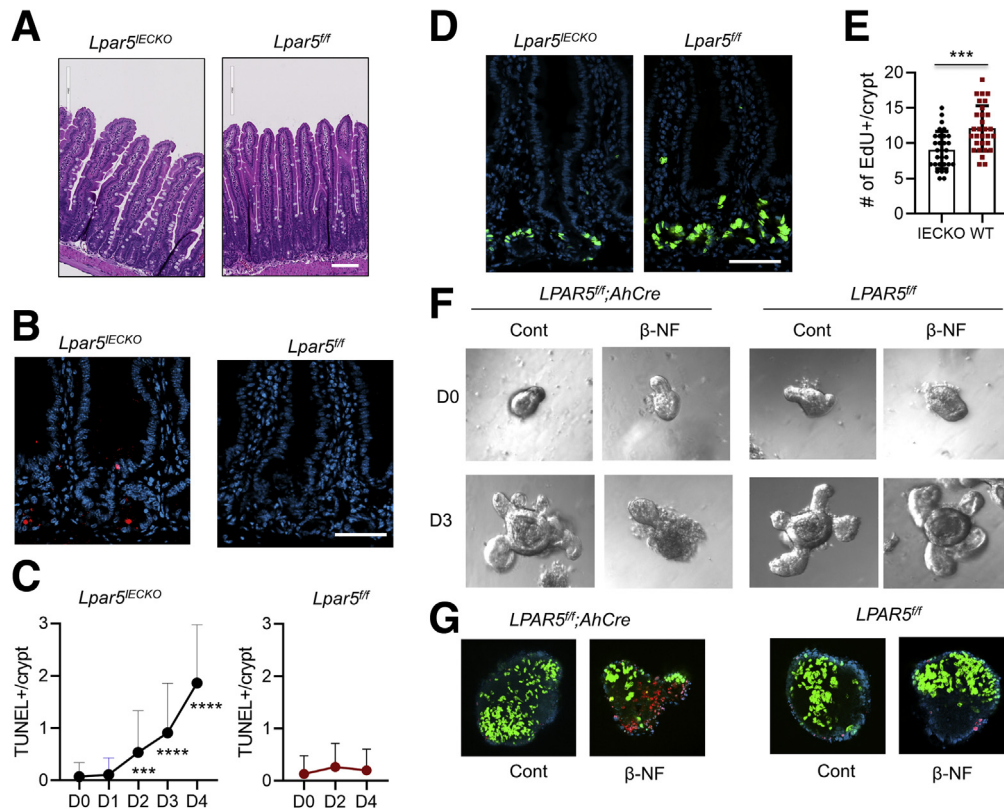


Figure 4. IEC-specific loss of *Lpar5* results in IEC death in mice and cultured enteroids. (A) *Lpar5^{ff}* and *Lpar5^{ff};AhCre* mice were treated by β -NF (80 mg/kg body weight) for 5 consecutive days and mice were euthanized 5 days after the last treatment. Representative hematoxylin and eosin images showing the histology of the small intestine of *Lpar5^{ff}* and *Lpar5^{IECKO}* mice. Scale bar = 100 μ m. (B) Representative IF images of TUNEL (red) staining in the intestinal sections of *Lpar5^{ff}* and *Lpar5^{IECKO}* mice. Scale bar = 100 μ m. (C) Time course of epithelial cell apoptosis was determined by treating *Lpar5^{ff};AhCre* mice (left, $n = 80$) or *Lpar5^{ff}* mice (right, $n = 30$) with β -NF for 5 consecutive days from day 0 (D0) to D5. TUNEL⁺ cell numbers per crypt were quantified each day. All data are presented as mean \pm SD. *** $P < .001$, **** $P < .0001$ compared with D0 by 1-way analysis of variance with Tukey's multiple comparison test. (D) Representative images of EdU⁺ cells in the crypts of *Lpar5^{IECKO}* and *Lpar5^{ff}* mice. Scale bar = 100 μ m. (E) Quantification of EdU⁺ cells per crypt (mean \pm SD) in *Lpar5^{ff}* and *Lpar5^{IECKO}* mice. $n = 30$. *** $P < .001$ by unpaired, 2-tailed t test. (F) Enteroids from *Lpar5^{ff}* and *Lpar5^{ff};AhCre* mice were treated with 1 μ M β -NF and images were taken before (0) and 72 hours of treatment. Representative of 3 experiments. (G) Representative EdU (green), TUNEL (red), and DAPI (blue) staining of enteroids are shown.

efficiency of *Lpar5^{KO}* enteroids was significantly increased in the presence of α -CXCL10 antibody, although it did not achieve a full recovery (Figure 7J).

CXCL10 mediates its effects through the activation of its receptor CXCR3.⁴⁶ CXCR3 is typically expressed in T cells and natural killer cells,⁴⁶ but mouse colonic epithelium also expresses CXCR3.¹² Quantitative reverse-transcription polymerase chain reaction (RT-PCR) analysis of *Lpar5^{ff}*, *Lpar5^{IECKO}*, and *Lpar5^{KO}* mouse enteroids confirmed the presence of CXCR3 in IECs, but interestingly, *Lpar5* deletion elevated CXCR3 mRNA levels (Figure 8A). We determined whether inhibition of CXCR3 can equally protect IECs by pretreating enteroids with a small molecule antagonist AMG487 (1 μ M) before deletion of *Lpar5*. Similar to neutralizing CXCL10, blockade of CXCR3 with the inhibitor prevented cell death and stimulated enteroid growth (Figure 8B).

To investigate whether neutralizing CXCL10 can protect mice in vivo, we administered α -CXCL10 antibody or control

IgG to *Lpar5^{KO}* mice according to the treatment scheme shown in Figure 9A. We observed that α -CXCL10 antibody prevented body weight loss in *Lpar5^{KO}* mice (Figure 9B). In addition, neutralization of CXCL10 prevented apoptosis in the intestinal crypts (Figure 9C and E) while promoting cell proliferation (Figure 9D and F). These effects are specific to *Lpar5^{KO}* mice as IgG or α -CXCL10 antibody had no effect on control mice (Figure 9G and H). Together, these results demonstrate that *Lpar5* loss induces IEC death in part through CXCL10-mediated cytotoxicity and blockade of CXCL10 can sufficiently prevent apoptotic death.

LPA₅-Expressing Splenocytes Protect *Lpar5*-Deficient IECs

Residing within the subepithelial compartment of the intestine are multiple populations of hematopoietic immune cells and mesenchymal cells. The phenotypic differences between *Lpar5^{IECKO}* and *Lpar5^{KO}* mice implied that these

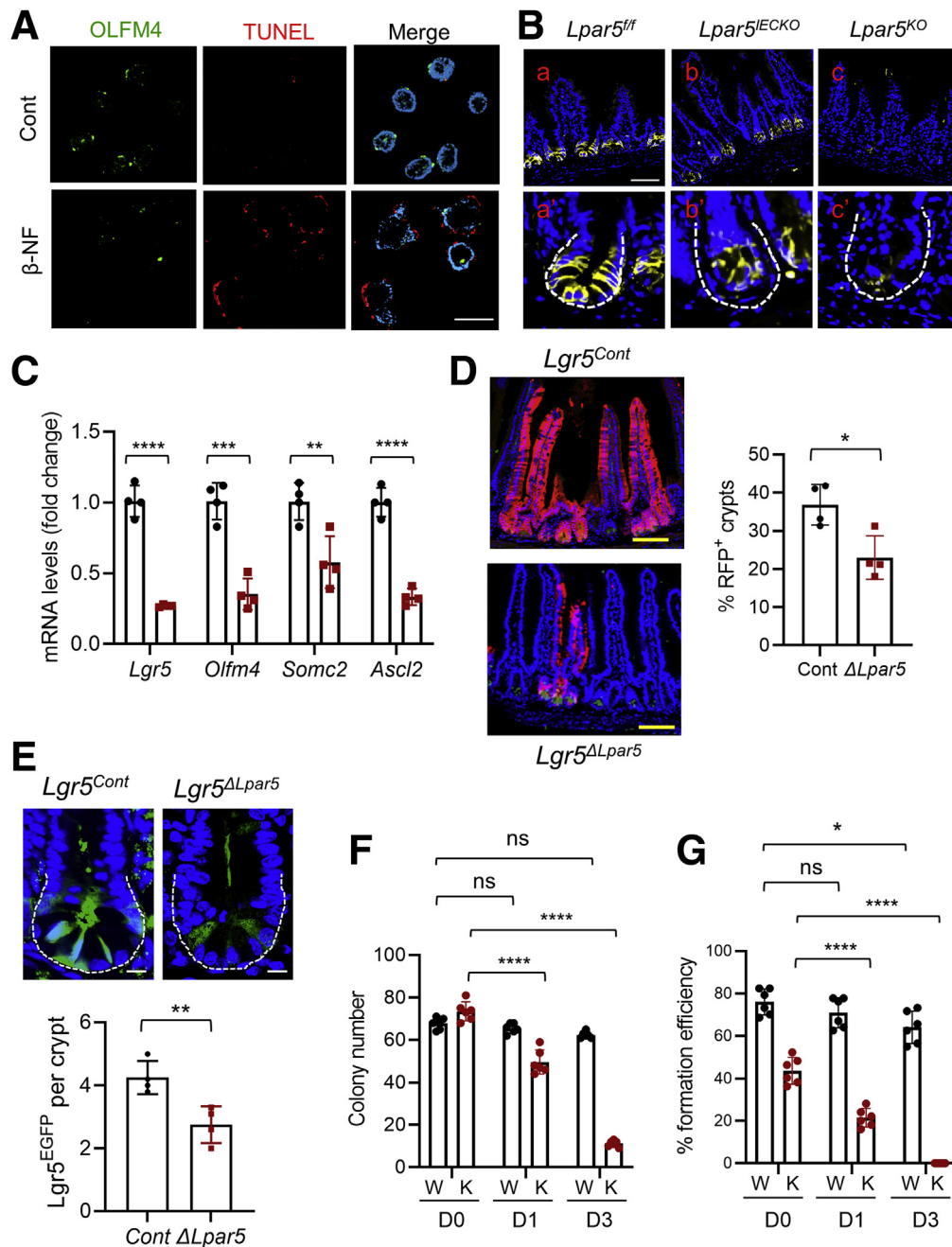


Figure 5. LPA₅ regulates intestinal stem cells. (A) The effect of *Lpar5* loss on ISCs was determined by IF microscopy of OLFM4 in enteroids treated with β -NF. IEC apoptosis was determined by TUNEL. Scale bar = 100 μ m. (B) OLFM4⁺ stem cells in the small intestinal crypts of *Lpar5^{fl/fl}*, *Lpar5^{IECKO}*, and *Lpar5^{KO}* mice were visualized by IF confocal microscopy. Representative of 3 experiments. Scale bar = 50 μ m. (C) Expression levels of ISC gene markers in isolated small intestinal crypts from *Lpar5^{fl/fl}* (black circle) and *Lpar5^{IECKO}* (red square) mice were determined by quantitative RT-PCR. n = 4. ***P* < .01, ****P* < .001, *****P* < .0001 by unpaired, 2-tailed *t* test. (D) Representative images of lineage tracing emanating from *Lgr5⁺* ISCs. Mice were treated with TAM for 5 days before collecting intestinal tissues. Scale bar = 100 μ m. Lineage trace events were identified as >5 tdT⁺ cells emanating from a crypt base and quantified. A total of >100 crypts per mouse were examined. n = 4 mice per genotype. Each data point represents the average of each mouse. ***P* < .01. (E) Representative images of EGFP (green) and DAPI (blue) of the intestinal crypts of *Lgr5^{Cont}* and *Lgr5 Δ Lpar5* mice are shown. Scale bar = 10 μ m. A total of >40 crypts were based on the presence of 3–5 Paneth cells per mouse examined. n = 4. Each data point represents the average number of EGFP⁺ cells per crypt in each mouse. ***P* < .01 by unpaired, 2-tailed *t* test. (F) *Lpar5^{fl/fl};Rosa-Cre^{ERT}* enteroids were plated on day 0 (D0) in the absence (W) or presence (K) of 4OHT. The number of viable enteroids was counted on D1 and D3. (G) Similar numbers of *Lpar5^{fl/fl};Rosa-Cre^{ERT}* enteroids in cultured in Matrigel were treated with 4OHT or sunflower oil for 16 hours. Enteroids dispersed mechanically and embedded on fresh layers of Matrigel (D0). Viable enteroids were counted. Data are presented as mean \pm SD. n = 6. **P* < .05; ****P* < .001; *****P* < .0001. ns indicates not significant by 2-way analysis of variance with Tukey's multiple comparison test.

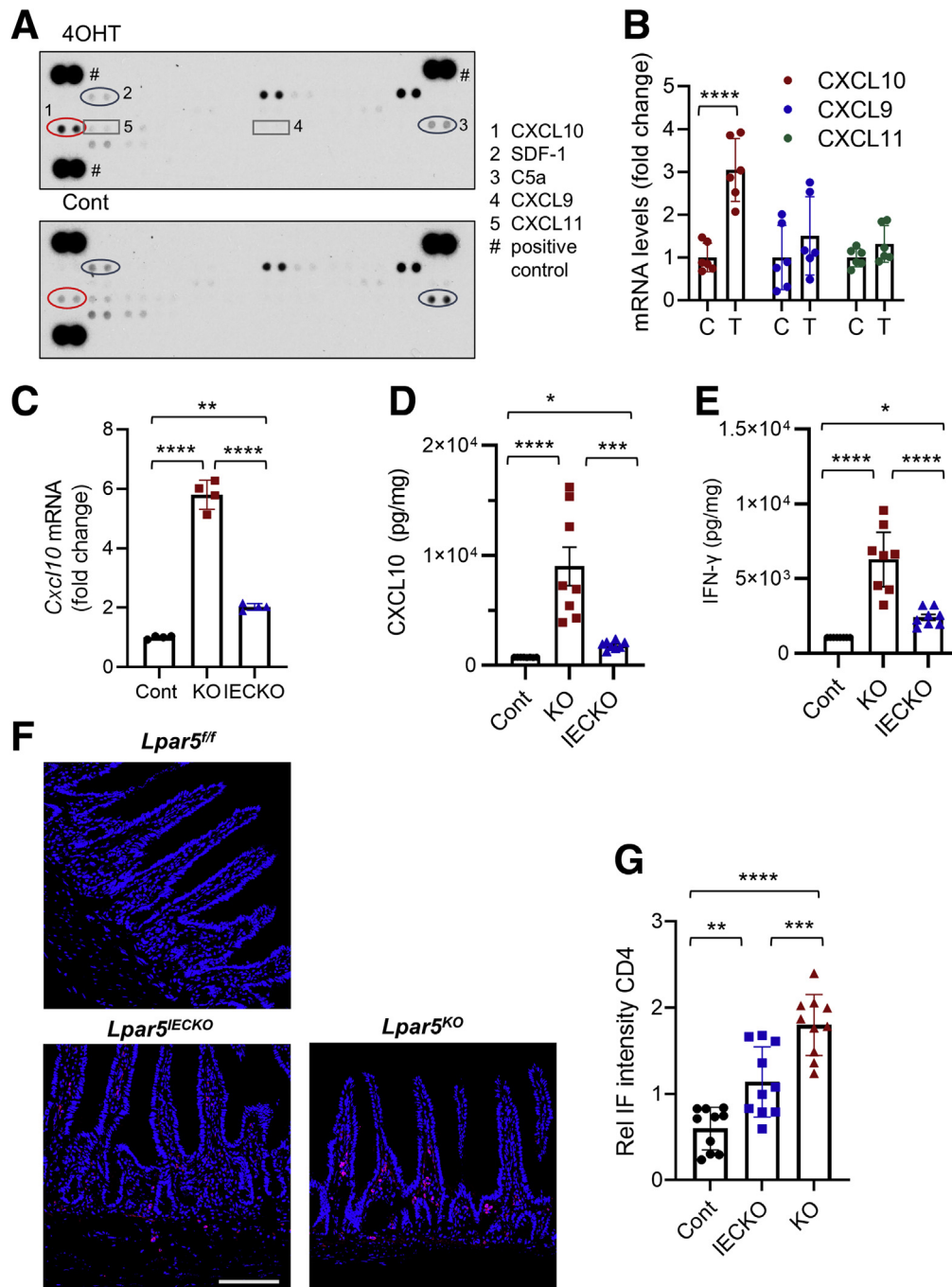
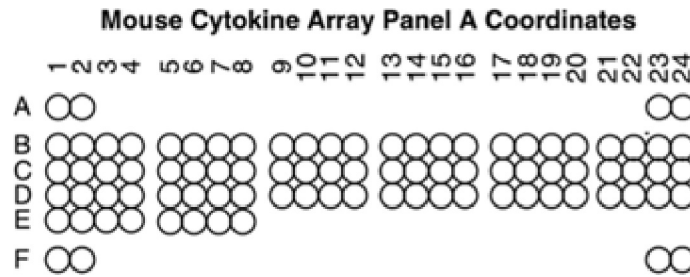


Figure 6. *Lpar5* loss increases the expression of CXCL10. (A) *Lpar5^{fl/fl}; RosaCre^{ERT}* enteroids were treated with 4OHT. The supernatant was harvested at 36 hours and used for a membrane-based cytokine array to identify cytokines altered by *Lpar5* loss. Representative blots from 2 independent experiments. (B) Quantitative RT-PCR comparing the expression levels of CXCL10, 9, and 11 in enteroids treated with 4OHT (T) or not (C). $n = 6$. $****P < .0001$ by unpaired, 2-tailed t test. (C) CXCL10 mRNA expression in *Lpar5^{fl/fl}*, *Lpar5^{KO}*, and *Lpar5^{IECKO}* mouse intestine was compared and presented as fold changes (mean \pm SD) relative to control mice. $n = 4$. $**P < .01$; $****P < .0001$ by 1-way analysis of variance with Tukey's multiple comparison test. (D, E) CXCL10 and IFN- γ expression levels in *Lpar5^{fl/fl}* (Cont), *Lpar5^{KO}* (KO), and *Lpar5^{IECKO}* (IECKO) mouse intestine were determined by ELISA. Representative of 2 experiments. $n = 8$. $*P < .05$, $***P < .001$, $****P < .0001$ by 1-way analysis of variance with Tukey's multiple comparison test. (F) Representative confocal IF images of CD4⁺ lymphocytes in the intestine. (G) Immunofluorescence (IF) intensity of CD4 was normalized to DAPI. $n = 8$. $**P < .01$, $***P < .001$, $****P < .0001$ by 1-way analysis of variance with Tukey's multiple comparison test.

Table 1. Densitometric Analysis of Mouse Cytokine Blot

Layout of the cytokine blot



Pixel density values of each cytokine

Coordinate	Target/Control	Control		KO		Mean Control	Mean KO	P Value
		1	2	1	2			
B1, B2	BLC (CXCL13/BCA-1)	0	0	0	0	0	0	
B3, B4	C5/C5a	228	219	140	174	223.5	157	.407631
B5, B6	G-CSF	0	0	0	0	0	0	
B7, B8	GM-CSF	0	0	0	0	0	0	
B9, B10	I-309 (CCL1/TCA-3)	0	0	0	0	0	0	
B11, B12	Eotaxin (CCL11)	0	0	0	0	0	0	
B13, B14	sICAM-1 (CD54)	233	225	214	227	229	220.5	.480965
B15, B16	FN-γ	96	81	58	44	88.5	51	.407631
B17, B18	IL-1a (IL-1F1)	0	0	0	0	0	0	
B19, B20	IL-1β (IL-1F2)	0	0	0	0	0	0	
B21, B22	IL-1ra (IL-1F3)	230	222	208	217	226	212.5	.480965
B23, B24	IL-2	0	0	0	0	0	0	
C1, C2	IL-3	0	0	0	0	0	0	
C3, C4	IL-4	0	0	0	0	0	0	
C5, C6	IL-5	0	0	0	0	0	0	
C7, C8	IL-6	0	0	0	0	0	0	
C9, C10	IL-7	0	0	0	0	0	0	
C11, C12	IL-10	0	0	0	0	0	0	
C13, C14	IL-13	0	0	0	0	0	0	
C15, C16	IL-12 p70	0	0	0	0	0	0	
C17, C18	IL-16	0	0	0	0	0	0	
C19, C20	IL-17	0	0	0	0	0	0	
C21, C22	IL-23	0	0	0	0	0	0	
C23, C24	IL-27	0	0	0	0	0	0	
D1, D2	CXCL10 (IP-10)	101	105	242	238	103	240	.004251
D3, D4	CXCL11 (I-TAC)	93	82	125	108	87.5	116.5	.420357
D5, D6	CXCL1 (KC)	62	31	86	75	46.5	80.5	.480965
D7, D8	M-CSF	0	0	0	0	0	0	
D9, D10	CCL2/MCP-1 (JE)	0	0	0	0	0	0	
D11, D12	CCL12 (MCP-5)	0	0	0	0	0	0	
D13, D14	CXCL9 (MIG)	0	0	0	0	0	0	
D15, D16	MIP-1a (CCL3)	0	0	0	0	0	0	
D17, D18	MIP-1β (CCL4)	0	0	0	0	0	0	
D19, D20	MIP-2 (CXCL2)	0	0	0	0	0	0	
D21, D22	RANTES (CCL5)	0	0	0	0	0	0	

Table 1. Continued

Coordinate	Target/Control	Pixel density values of each cytokine						P Value
		Control		KO		Mean Control	Mean KO	
		1	2	1	2			
D23, D24	SDF-1 (CXCL12)	126	168	68	83	147	75.5	.413314
E1, E2	TARC (CCL17)	0	0	0	0	0	0	
E3, E4	TIMP-1	143	126	85	67	134.5	76	.32022
E5, E6	TNF- α	68	72	55	32	70	43.5	.480965
E7, E8	TREM-1	0	0	0	0	0	0	

KO, knockout;

nonepithelial cells modulate the survival of ISCs and TA cells in a LPA₅-dependent manner. To test this hypothesis, we isolated splenocytes from the spleen of *Lpar5*^{f/f} (WT) and *Lpar5*^{KO} mice and co-cultured them with *Lpar5*^{f/f}; *Rosa-Cre*^{ERT} enteroids. In comparison with enteroids treated with 4OHT alone (Figure 10A, i and i'), enteroids co-cultured with WT splenocytes displayed the formation of crypt-like budings (Figure 10A, ii and ii'), indicating that the growth of enteroids was sustained by WT splenocytes. This protective effect was not observed when co-cultured with *Lpar5*^{KO} splenocytes (Figure 10A, iii and iii'), demonstrating that *Lpar5*^{KO} splenocytes lost the ability to protect epithelial cells. These differences were confirmed by decreased levels of TUNEL staining together with increased EdU staining in enteroids co-cultured with WT splenocytes but not with *Lpar5*^{KO} splenocytes (Figure 10B). On the contrary, the growth (Figure 10C) and survival of WT enteroids (percentages of surviving enteroids on D2/D0 were 97.8 ± 2.9% without splenocytes, 98.1 ± 3.7% with WT splenocytes, and 98.1 ± 4.4% with *Lpar5*^{KO} splenocytes) were not affected by WT or *Lpar5*^{KO} splenocytes. Further, we observed increased OLFM4 immunofluorescence labeling (Figure 10D) and ISC-specific *Lgr5*, *Olfm4*, *Smoc2*, and *Ascl2* mRNA expression (Figure 10E) in enteroids co-cultured with WT splenocytes, demonstrating the protection of ISCs by WT splenocytes.

Although WT splenocytes protect *Lpar5*^{KO} enteroids, how this protective effect is manifested is not clear. Recent studies have demonstrated that T cells in the crypt compartment modulates the fate of intestinal stem cells.^{3,47} IL-10 secreted by CD4⁺ T helper cells, for example, promotes stem cell renewal.³ Interestingly, we observed that *Il-10* mRNA levels were lower in *Lpar5*^{KO} splenocytes compared with WT splenocytes (Figure 11A). Therefore, we postulated that IL-10 secreted by lymphocytes might prevent IEC death by mitigating CXCL10-dependent cytotoxic effects. In line with this postulation, we found that the expression levels of *Cxcl10* mRNA in *Lpar5*^{KO} enteroids co-cultured with WT splenocytes were significantly diminished compared with those co-cultured with *Lpar5*^{KO} splenocytes (Figure 11B). To assess a direct effect of IL-10 on CXCL10, we treated *Lpar5*^{KO} enteroids with IL-10 for 2 days. We observed that *Cxcl10* mRNA expression was significantly diminished by IL-10 (Figure 11C). Further, IL-10 protected

Lpar5^{KO} enteroids so that there were increased numbers of viable enteroids in the presence of IL10 (Figure 11D). Consistent with the notion that IL-10 antagonizes CXCL10, addition of IL-10 to the coculture containing *Lpar5*^{KO} splenocytes decreased *Cxcl10* mRNA expression (Figure 11E) (KO vs KO+IL10). Additionally, IL-10 increased cell proliferation, while preventing cell death (Figure 11F–H) (KO vs KO+IL10). To prove that IL-10 released by WT splenocytes indeed protects *Lpar5*^{KO} enteroids, *Lpar5*^{KO} enteroids were co-cultured with WT splenocytes in the presence or absence of α -IL-10 antibody. Neutralizing IL-10 increased *Cxcl10* expression (Figure 11E) (WT vs WT+ α IL10), which blocked cell proliferation (Figure 11H, WT vs WT+ α IL10) while promoting apoptosis (Figure 11G) (WT vs WT+ α IL10). Together, these data suggest that IL-10 secreted by WT lymphocytes protect *Lpar5*-deficient crypt epithelial cells by suppressing the cytotoxic effects of CXCL10.

Discussion

In this study, we demonstrate that LPA₅ plays a critical role in the maintenance of stem cells and TA cells in the intestine. Loss of *Lpar5* impairs the epithelial renewal, resulting in near complete atrophy of the intestinal tract. Using intestinal enteroids, we show that LPA₅ is necessary to support the survival of ISCs and TA cells. However, IEC-specific *Lpar5* deletion was not sufficient to cause mucosal damage in the mouse intestine despite increased apoptosis in the intestinal crypts. Our data subsequently showed that lymphocytes protect ISCs and TA cells in a LPA₅-dependent modulation of CXCL10 expression.

At the bottom of each crypt in the intestine, about a dozen *Lgr5*⁺ stem cells reside intercalated with the Paneth cells.³⁴ In addition to *Lgr5*⁺ stem cells, there are reserved stem cells, marked by enriched expression of *Bmi1* or *Lrig1*, that are thought to regenerate actively proliferating *Lgr5*⁺ stem cells following severe intestinal crypt damage.⁴⁸ Previous single-cell sequencing analyses have shown the presence of *Lpar5* mRNA in mouse and human *Lgr5*⁺ ISCs.^{49,50} In addition, *Lpar5* mRNA was detected in *Lrig1*⁺ stem cells.⁴⁹ We provide here experimental evidence that LPA₅ regulates ISCs. First, IEC-specific deletion of *Lpar5* resulted in decreased *Olfm4*⁺ stem cell numbers in the

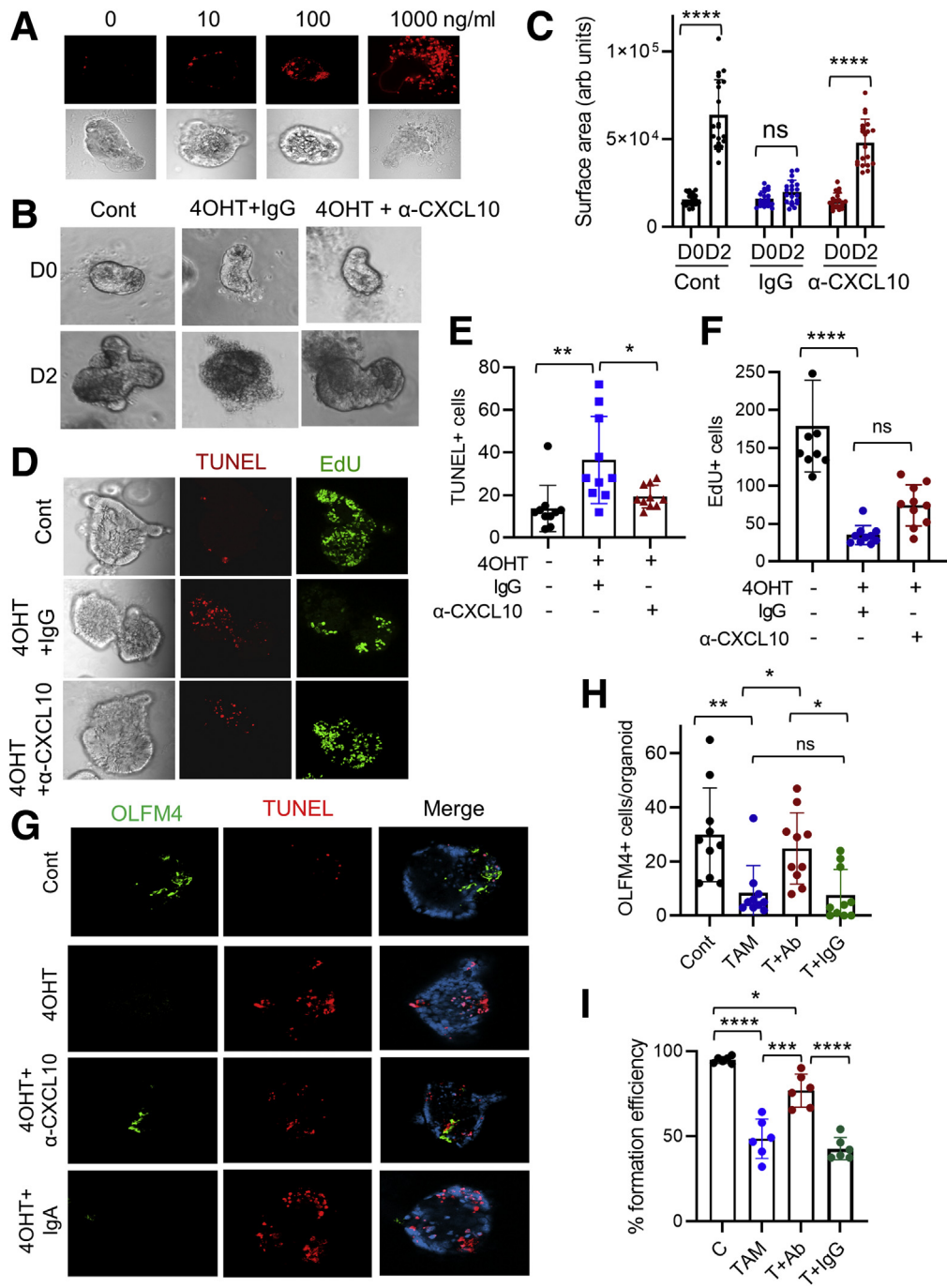


Figure 7. Neutralizing anti-CXCL10 antibody attenuates IEC apoptosis. (A) Enteroids derived from WT mouse intestine were incubated with different concentrations of recombinant CXCL10. Representative images of TUNEL and bright field are shown. (B) Enteroids from *Lpar5^{fl/fl}; RosaCre^{ERT}* mice were treated with 4OHT in the presence of anti-CXCL10 (α -CXCL10) antibody or isotype control antibody (IgG). Enteroids untreated with 4OHT (Cont) were used for comparison. Representative of 3 experiments. (C) The growth of enteroids in the presence of IgG or α -CXCL10 antibody was quantified by determining the surface area of enteroids using ImageJ. All data are presented as mean \pm SD. $n = 20$. $****P < .0001$. (D) Enteroids on day 1 (D1) were stained for apoptosis (TUNEL) and proliferation (EdU). (E, F) Quantification of TUNEL⁺ and EdU⁺ cells are shown. $n = 10$. $*P < .05$, $**P < .01$, $****P < .0001$, ns not significant by 1-way analysis of variance with Tukey's multiple comparison test. (G) Representative OLFM4 and TUNEL IF images of enteroids from 3 experiments are shown. (H) Quantification of OLFM4⁺ cells per enteroids. $n = 10$. $*P < .05$, $**P < .01$, ns not significant. (I) Colony-forming efficiencies of enteroids were determined. Data are presented as mean \pm SD. $n = 6$. $*P < .05$; $***P < .001$; $****P < .0001$. ns indicates not significant by 2-way analysis of variance with Tukey's multiple comparison test.

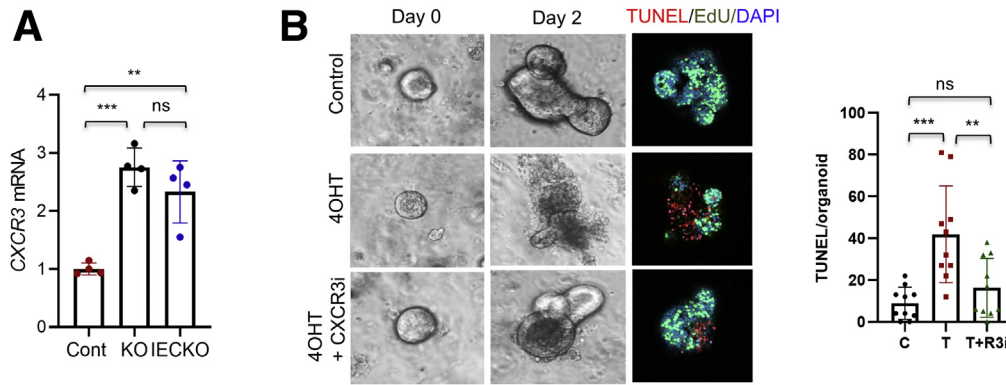


Figure 8. Blockade of CXCR3 inhibits epithelial cell apoptosis. (A) CXCR3 mRNA expression was determined in *Lpar5^{ff}*, *Lpar5^{KO}*, and *Lpar5^{IECKO}* organoids. $n = 4$. $**P < .01$, $***P < .001$. (B) Representative images of organoids treated with 4OHT or 4OHT plus CXCR3 inhibitor AMG487. Immunofluorescence images of TUNEL and DAPI on day 2 are shown. TUNEL⁺ cells per organoids are quantified on the right. Data are presented as mean \pm SD. $n = 10$. $**P < .01$; $***P < .001$. ns indicates not significant by 1-way analysis of variance with Tukey's multiple comparison test.

intestine. Second, *Lpar5* loss in *Lgr5⁺* ISCs mitigated lineage tracing emanating from *Lgr5⁺* stem cells and decreased the number of EGFP-expressing *Lgr5⁺* ISCs. Third, *Lpar5* loss decreased the clonogenicity of enteroids that requires functional ISCs. It has been shown that acute ablation of *Lgr5⁺* ISCs does not compromise epithelial integrity because other cells replenish the *Lgr5⁺* ISCs.^{36,51} On the other hand, a recent study by the Barker group showed that higher ablation efficiency of *Lgr5⁺* ISCs compromises small intestinal integrity and impairs intestinal homeostasis.⁵² We found in this study that the levels of crypt cell apoptosis in *Lpar5^{IECKO}* mouse small intestine were lower compared to *Lpar5^{KO}* intestine. Therefore, we inferred that the phenotypic difference between *Lpar5^{KO}* and *Lpar5^{IECKO}* intestine reflect the differential extent of ISCs and TA cell ablation.

A recent study by Konno et al²⁰ demonstrated the role of LPA on the growth of enteroids. LPA can substitute EGF to promote the growth and differentiation of IECs in enteroids.²⁰ Our previous studies have shown that LPA₅ transactivates the EGF receptor,^{53,54} but the findings in the current study indicate that the loss of LPA₅ function in *Lpar5^{KO}* or *Lpar5^{ΔIEC}* enteroids cannot be explained solely by the loss of EGF receptor activity because EGF was present in the culture media. Single cell-sequencing analyses have shown the presence of *Lpar5* mRNA is multiple types of cells, including ISCs, TA cells, mature enterocytes, macrophages, and lymphocytes.⁵⁰ LPA regulates major signaling pathways, including the Wnt, PI3K, mitogen-activated protein kinase, and Hippo-YAP pathways, which are required for the maintenance of stem cells.^{55–57} Given the expression of *Lpar5* in ISCs and TA cells, we speculate that the loss of LPA₅-mediated signaling disrupts the balance in cellular signaling that maintains the stem cell niches, rather than specifically injuring ISCs or progenitors. Future studies are required to decode LPA₅-mediated cellular signaling that regulates ISC and progenitors.

Previous studies have shown that IECs are a major source of CXCL10.^{7,8,58} In the current study, we found upregulation of CXCL10 expression by *Lpar5* loss in both

intestinal enteroids and mouse intestine. In addition, the CXCR3 mRNA levels in IECs were found to be elevated by *Lpar5* loss. Although CXCL9, CXCL10, and CXCL11 share the same receptor, CXCR3, we did not find CXCL9 or CXCL11 expressed altered by *Lpar5* loss. Previous studies showed that these chemokines are differentially expressed in different pathological conditions, suggesting that they have nonredundant functions.⁴⁶ We found that recombinant CXCL10 induced epithelial cell apoptosis in mouse intestinal enteroids, consistent with previous studies demonstrating the cytotoxic effects of CXCL10 on several types of cells, including neurons,³⁸ lymphocytes,³⁹ and hepatocytes.⁴⁰ Importantly, neutralizing CXCL10 signaling prevented cell death induced by *Lpar5* loss, demonstrating that the upregulation of CXCL10 is a major cause of LPA₅-dependent IEC death. Consistent with our data, blockade of CXCL10 was shown to enhance crypt cell survival and protect mice from acute colitis.^{11,12} CXCL10 blockade impairs the recruitment of lymphocytes into the brain⁵⁹ and colon,¹¹ whereas increased CXCL10 secretion is associated with enhanced T cell infiltration.^{60,61} We observed increased levels of both CXCL10 and IFN- γ along with increased infiltration of T cells in *Lpar5^{KO}* mice compared with *Lpar5^{IECKO}* mice. In keeping with our data, increased levels of IFN- γ and CXCL10 are observed in many T helper-1-type inflammatory diseases, including diabetes,⁶² multiple sclerosis,⁵⁹ and celiac disease.⁸ The direct effect of IFN- γ on CXCL10 production has been demonstrated in patients with systemic lupus erythematosus⁶³ and in mouse colon.⁶⁴

The crypt base region where ISCs and their niche reside is a primary site of T cell invasion within the intestinal mucosa during immune-mediated GI damage,⁴⁷ and several studies have shown important roles that immune cells play in ISC homeostasis.^{3,47} Biton et al³ recently reported that regulatory T cells stimulate stem cell renewal via secretion of IL-10. In addition, IL-10 was shown to suppress *Cxcl10* transcription.⁶⁵ Remarkably, *Il-10* mRNA expression levels differed between WT and *Lpar5^{KO}* splenocytes, and our data showed that WT splenocytes or addition of IL-10

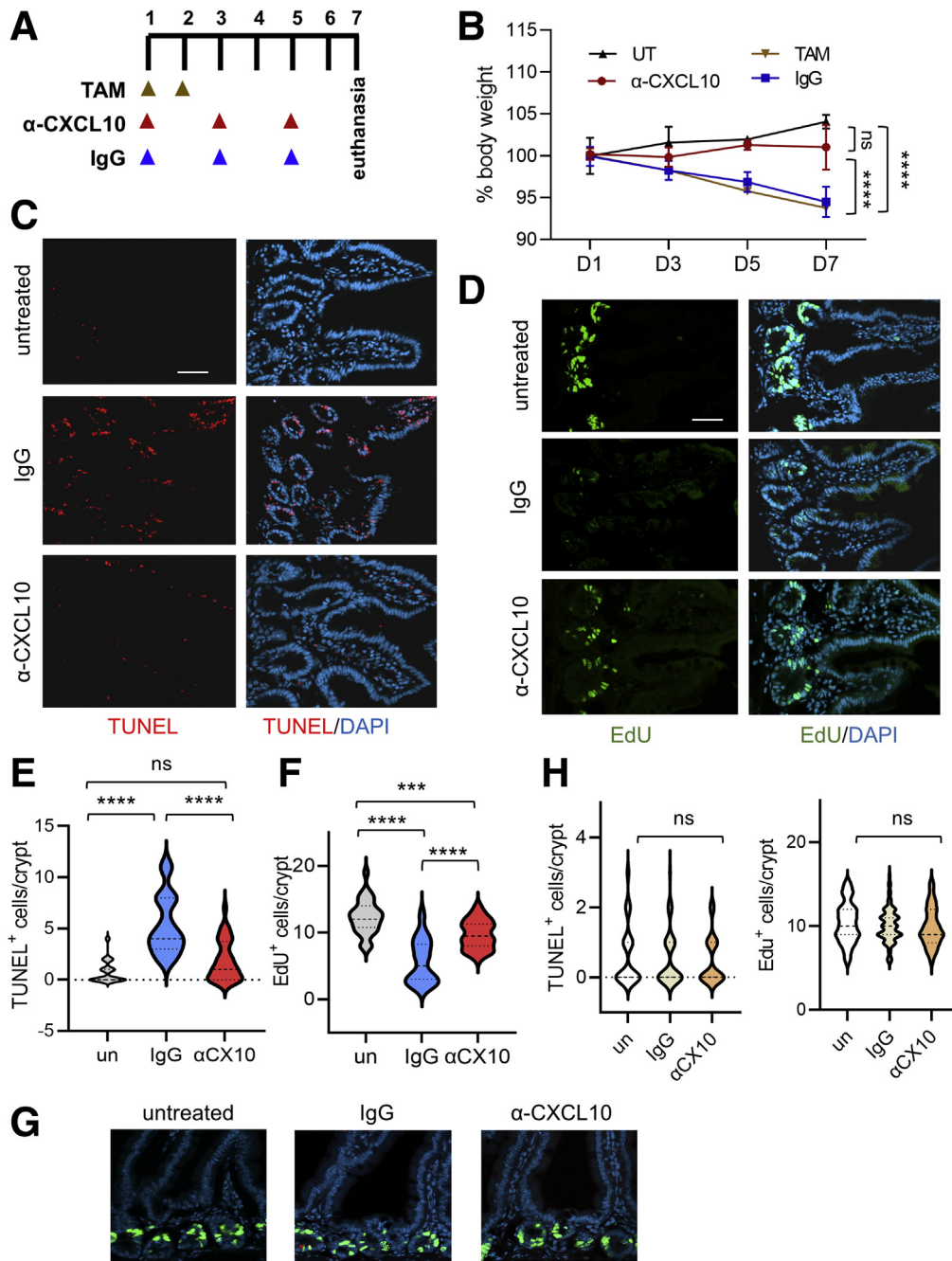


Figure 9. CXCL10 neutralization protects *Lpar5*^{KO} mice. (A) *Lpar5*^{ff}, *Rosa-Cre*^{ERT} mice treated with TAM for 2 days were administered α -CXCL10 or control IgG as indicated in the scheme. (B) Body weights expressed as percent of the initial body weight are shown. UT indicates mice not treated with TAM. TAM indicates treated with TAM. n = 4. Representative of 3 independent experiments. ****P < .0001 vs IgG. ns, α -CXCL10 vs UT. (C, D) Representative IF images showing TUNEL⁺ and EdU⁺ cells in intestinal sections. Scale bar = 50 μ m. (E, F) Quantification of TUNEL⁺ or EdU⁺ cells per crypt are shown. There were \geq 30 crypts. Data are presented as mean \pm SD. n = 30. ***P < .001, ****P < .0001, ns not significant by 1-way analysis of variance with Tukey's multiple comparison test. (G) Representative IF images of TUNEL and EdU labeling in control *Lpar5*^{ff} mice treated with IgG or α -CXCL10 antibody are shown. (H) Quantification of the number of TUNEL⁺ and EdU⁺ cells per crypt in *Lpar5*^{ff} mice is shown. n > 30.

downregulated *Cxcl10* expression and protected enteroids from apoptosis. Moreover, neutralizing IL-10 lowered *Cxcl10* expression and blocked the protective effects of WT splenocytes, affirming the protective effects of IL-10. Our data therefore indicate that WT lymphocytes in *Lpar5*^{IECKO} mice produce IL-10 that antagonizes CXCL10 and protects ISCs and progenitors. By contrast, IL-10 expression in LPA₅-deficient lymphocytes in *Lpar5*^{KO} mice was low and unable to modulate CXCL10, and hence failed to prevent epithelial ablation. Interestingly, LPA₅ was shown to have a strong inhibitory effect on tumor necrosis factor α (TNF- α) production by macrophages via upregulation of IL-10.⁶⁶

However, others have shown that pharmacological inhibition of LPA₅ in microglia cells inhibits secretion of proinflammatory cytokines in microglia cells,⁶⁷ indicating that the role of LPA₅ in immunity may be context dependent.

One notable finding of the current study is the striking difference between constitutive deletion of *Lpar5* vs conditional deletion. Constitutive or germline deletion of a gene often results in severe phenotype revealing the critical importance of the gene in developmental process. For example, constitutive deletion of the *Enpp2* gene encoding autotaxin results in prenatal demise owing to the vascular defects in embryos,⁶⁸ but similar lethal effects are not

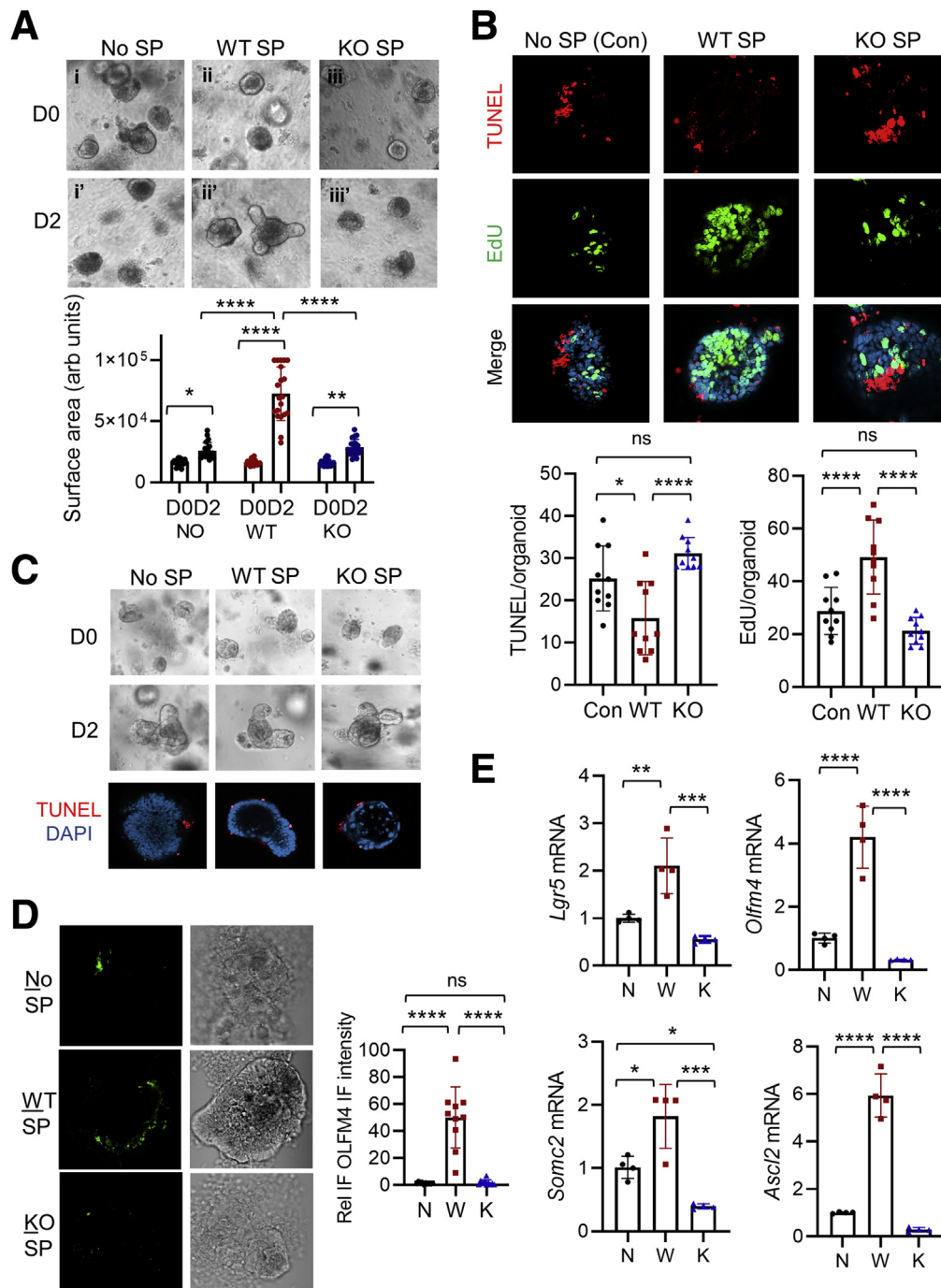


Figure 10. WT splenocytes (SP) protect stem cells and progenitors from *Lpar5*-dependent apoptosis. (A) Enteroids were co-cultured with SP from WT or *Lpar5*^{KO} (KO) mice. Representative images from 3 experiments are shown. The size of enteroids was quantified by determining the surface area of enteroids using ImageJ. $n = 20$. * $P < .05$, ** $P < .01$, **** $P < .0001$ by 2-way analysis of variance with Tukey's multiple comparison test. (B) Apoptosis and proliferation of IECs were determined by immunofluorescence microscopy. Apoptotic (TUNEL) and proliferating (EdU) cells were quantified. Data are presented as mean \pm SD. $n = 10$. * $P < .05$, **** $P < .0001$. (C) Growth of WT enteroids in the presence of WT or *Lpar5*^{KO} splenocytes was determined. Representative phase-contrast and confocal TUNEL IF images of enteroids are shown. (D) Representative confocal immunofluorescence microscopic images of enteroids stained for OLFM4 are shown. Relative IF intensity of OLFM4 was quantified below. $n = 10$. **** $P < .0001$. (E) Expression levels of stem cell markers, *Lgr5*, *Olfm4*, *Somc2*, and *Ascl2*, were determined. N indicates *Lpar5*^{KO} enteroids alone; W indicates *Lpar5*^{KO} enteroids co-cultured with WT splenocytes; K indicates *Lpar5*^{KO} enteroids co-cultured with *Lpar5*^{KO} splenocytes. Data are presented as mean \pm SD. * $P < .05$, ** $P < .01$, *** $P < .001$, **** $P < .0001$ by 1-way analysis of variance with Tukey's multiple comparison test. ns indicates not significant by 1-way analysis of variance with Tukey's multiple comparison test.

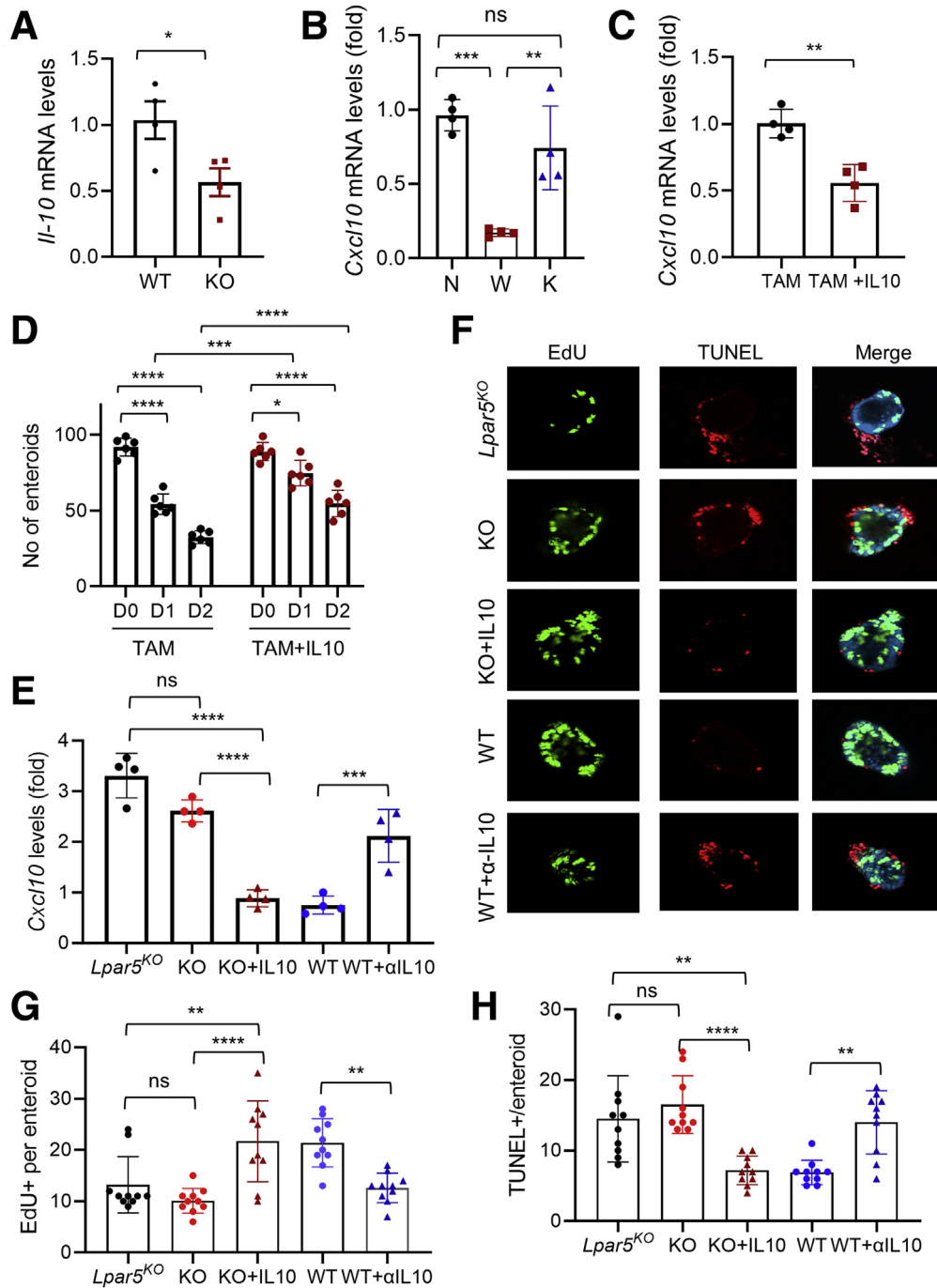


Figure 11. Decreased IL-10 expression in *Lpar5*-deficient splenocytes. (A) *Il-10* mRNA expression was determined in WT and *Lpar5*^{KO} (KO) splenocytes. n = 3. **P* < .05. (B) The effects on splenocytes on *Cxcl10* mRNA expression in *Lpar5*^{KO} organoids were determined. N indicates no splenocytes; W indicates co-cultured with WT splenocytes; and K indicates co-cultured with *Lpar5*^{KO} splenocytes. n = 4. ***P* < .01; ****P* < .001. (C) *Cxcl10* mRNA levels were determined in *Lpar5*^{KO} organoids with or without IL-10. n = 4. ***P* < .01. (D) *Lpar5*^{KO} enteroids were cultured with or without 100 ng/mL IL-10. Numbers of viable enteroids were counted. n = 6. ****P* < .001; *****P* < .0001. (E) *Cxcl10* expression levels were determined in *Lpar5*^{KO} enteroids co-cultured with *Lpar5*^{KO} splenocytes (KO), *Lpar5*^{KO} splenocytes+IL10 (KO+IL10), WT splenocytes (WT), or WT splenocytes+α-IL10 antibody (WT+αIL10). n = 4. ****P* < .001; *****P* < .0001. (F) Representative confocal IF microscopic images of enteroids stained for EdU or TUNEL under the same conditions described previously. Quantification of (G) EdU⁺ or (H) TUNEL⁺ per enteroid are shown. n = 10. ***P* < .01; ****P* < .001; *****P* < .0001. ns indicates not significant by 1-way analysis of variance with Tukey's multiple comparison test.

observed by postnatal loss of *Enpp2*.^{69,70} On the other hand, mutations in germline cells are less frequent than spontaneous mutations and genetic compensations may mask a phenotype of a germline defect.⁷¹ Unlike the phenotype of *Lpar5*^{KO} mice, constitutive deletion of *Lpar5* does not cause a change in a baseline phenotype.²⁷ The absence of a gross phenotype by constitutive *Lpar5* ablation suggests that LPA₅ functions in the developing embryos are masked by yet unknown compensatory responses.

Accumulating evidence links aberrant LPA signaling to inflammation in the gut.^{70,72,73} Recent genome-wide association studies have identified a single nucleotide polymorphism in G protein-coupled receptor GPR35 (rs4676410) among patients with IBD.^{74,75} Importantly, LPA has been identified as an endogenous ligand of GPR35, associating aberrant LPA-mediated signaling to the pathogenesis of IBD.⁷⁶ More recently, loss of GPR35 signaling in CX3CR1⁺ macrophages has been shown to exacerbate dextran sodium sulfate-induced colitis in mice by altering TNF synthesis.⁷⁷ We have shown recently that the absence of LPA₅ in IECs compromises the epithelial barrier function and increases the susceptibility to dextran sodium sulfate-induced colitis.²⁴ However, despite the striking phenotypic changes observed in mice lacking LPA₅, there is no evidence linking mutations in *Lpar5* gene to GI disorders in humans. Interestingly, a *Lpar5* genetic variant is associated with increased levels of triglyceride and high density-lipoprotein cholesterol in circulation that increase the risk of coronary heart disease.⁷⁸ Patients with IBD have an elevated risk of cardiovascular morbidity relative to the general population,^{79–81} but whether the *Lpar5* variant is present in the subset of IBD patients with hyperlipidemia is not yet known.

We demonstrate here that inducible deletion of LPA₅ causes a major defect in the GI system by inducing apoptotic loss of stem cells and TA cells, which compromises the regenerative capacity of the GI tract, resulting in increased morbidity. However, the maintenance of intestinal epithelium by LPA₅ is orchestrated between the crosstalk between the epithelial stem cells or progenitors and lymphocytes in the crypt compartment that regulate anti-inflammatory IL-10 while keeping cytotoxic CXCL10 in check.

Materials and Methods

Mice

Lpar5^{f/f} mice generated by the Mouse Transgenic Core at Emory University were previously described.²³ C57BL/6, *Rosa26-Cre*^{ERT}, *Lgr5-EGFP-ires-Cre*^{ERT2}, and *Rosa26-tdTomato* mice were obtained from the Jackson Laboratory (Bar Harbor, ME) and housed in specific pathogen-free conditions. *AhCre* mice³² were provided by Dr. Douglas J. Winton (Cancer Research UK Cambridge Institute). *Lpar5*^{f/f} mice were bred with *Rosa-Cre*^{ERT} mice and *AhCre* to obtain *Lpar5*^{f/f};*RosaCre*^{ERT} (*Lpar5*^{KO}) and *Lpar5*^{f/f};*AhCre* (*Lpar5*^{IECKO}) mice, respectively. *Lpar5*^{f/f} mice bred with *Lgr5-EGFP-ires-Cre*^{ERT2} mice, followed by crossing with *Rosa26-tdTomato* mice, resulting in *Lpar5*^{f/f};*Lgr5-EGFP-ires-Cre*^{ERT2};*Rosa26-tdTomato* (*Lgr5*^{Lpar5}) mice and control

Lgr5-EGFP-ires-Cre^{ERT2};*Rosa26-tdTomato* (*Lgr5*^{Cont}). All mice were kept on ad libitum normal chow and water. To induce recombination, mice were injected intraperitoneally with TAM dissolved in corn oil (10 mg/mL; Sigma-Aldrich, St. Louis, MO) at 40 mg/kg for 5 consecutive days unless otherwise noted. *Lpar5*^{f/f};*AhCre* mice were given intraperitoneal injections of 80 mg/kg β-NF dissolved in corn oil (8 mg/mL) for 5 consecutive days. For all experiments, gender-matched mice between the ages of 8 and 12 weeks were used. To determine the number of actively dividing cells in the intestine, mice were injected with EdU (20 mg/kg body weight) by intraperitoneal injection 2 hours prior to euthanasia. All animal experiments were conducted under approval by the Institutional Animal Care and Use Committee of Emory University and in accordance with the National Institutes of Health's Guide for the Care and Use of Laboratory Animals.

Intestinal Crypt Isolation and 3-Dimensional Culture of Enteroids

Mouse small intestinal crypts were cultured as previously described.³¹ In brief, isolated small intestine was cut longitudinally and washed with cold phosphate-buffered saline (PBS). Crypts were incubated for 1 hour at room temperature in Gentle Cell Dissociation Reagent (STEMCELL Technologies, Vancouver, Canada) and released from tissue by gentle agitation. Crypts were then passed through a 70-μm cell strainer and the crypt fraction was enriched by centrifugation. Crypts were embedded in Matrigel and cultured in growth media (50% advanced Dulbecco's modified Eagle medium/F-12, 50% L-WRN, 10% fetal bovine serum [FBS], N-2 media supplement, B-27 supplement, 100 units/mL penicillin, and 0.1 mg/mL streptomycin). Media were replenished every 2–3 days.

Enzyme-Linked Immunosorbent Assay

Mouse jejunum sections were harvested and washed with ice-cold PBS for 3 times. A total of 20 mg of tissues were resuspended in 700 μL of lysis buffer (20 mM Tris-HCl [pH 7.5], 150 mM NaCl, 1 mM Na₂EDTA, 1 mM EGTA, 1% Triton, 2.5 mM sodium pyrophosphate, 1 mM beta-glycerophosphate, 1 mM Na₃VO₄, 1 μg/mL leupeptin, protease inhibitor cocktail, 1 mM phenylmethylsulfonyl fluoride). Samples were sonicated and centrifuged at 13,000 rpm for 15 minutes at 4 °C. Cleared supernatants were diluted 1:10 or 1:100 using assay buffer and used for enzyme-linked immunosorbent assay (ELISA) assay using the Mouse IFN-γ ELISA kit and Mouse CXCL10 ELISA kit (RayBiotech, Norcross, GA) according to the manufacturer's instruction.

Treatment of Enteroids With Anti-CXCL10 Antibody and CXCR3 Inhibitor

Enteroids were treated with 1 μM 4OHT alone or together with anti-CXCL10 antibody (AF-466-NA, 100 ng/mL; R&D Systems, Minneapolis, MN). As a control, isotype IgG antibody (31933; Thermo Fisher Scientific, Waltham,

MA) was used. To block CXCR3, enteroids were treated with AMG487 (10 μ M; Cayman Chemical, Ann Arbor, MI) or dimethyl sulfoxide as a control. EdU and TUNEL staining was processed as described above.

Treatment of Mice With Anti-CXCL10 Antibody

Lpar5^{ff};RosaCre^{ERT} mice, gender and age matched, were given TAM (100 mg/kg body weight/d) for 2 consecutive days. Group 1 and group 2 were administered 100 μ g anti-mouse CXCL10 antibody or isotype IgG, respectively, on alternate days for 3 times. Group 3 received the same volume of PBS. On day 7, each mouse was administered EdU and euthanized 2 hours later.

Co-Culture of Enteroids With Splenocytes

A single cell suspension of lymphocytes from spleen was generated as previously described.⁸² Briefly, freshly isolated spleen from *Lpar5^{ff}* or *Lpar5^{KO}* mice placed in a 60 mm petri dish with ice-cold 5 mL Hank's Balance Salt Solution buffer and was minced into small pieces with a razor blade. Excised spleen pieces were mashed through a sterile 100 μ m strainer with the plunger of a 1 mL syringe. Cells passed through the strainer were centrifuged at 500 *g* for 5 minutes at 4 °C. The cell pellet was resuspended in 5 mL of cold 1 \times red blood cell lysis buffer (eBioscience, San Diego, CA) and incubated at room temperature for 3–4 minutes. Cells were washed with 10 mL ice-cold PBS and centrifuged at 500 *g* for 5 minutes at 4 °C. The cell pellet was resuspended in complete Dulbecco's modified Eagle medium media (10% FBS 10 mm HEPES, pH 7-4, 10 mM L-glutamine, plus 10% FBS 100 U/mL of penicillin, and 100 μ g/mL of streptomycin). Cell numbers were counted using a hemocytometer. At the same time, intestinal crypts were isolated from a 6- to 8-week-old *Lpar5^{ff};RosaCre^{ERT}* mouse and approximately 500 crypts were embedded in Matrigel. Splenocytes were activated by using 10 μ g/mL lipopolysaccharide (eBioscience). Activate splenocytes were added to enteroids at the ratio of 100,000 splenocytes to 500 crypts.

Treatment of Enteroids With IL-10 or Anti-IL-10 Antibody

Enteroids were treated with 1 μ M 4OHT alone or together with 100 ng/mL mouse IL-10 (417-ML; R&D Systems). In some experiments, enteroids were co-cultured with splenocytes with or without rat anti-mouse IL-10 antibody (MAB417; R&D Systems).

Quantitative RT-PCR

Intestinal mucosal scrapes and cultured enteroids were harvested to extract total RNA with the RNeasy Mini kit (Qiagen, Hilden, Germany). One microgram of total RNA was used for cDNA synthesis using the First Strand cDNA Synthesis Kit (Thermo Fisher Scientific) according to the manufacturer's instruction. Quantitative PCR was performed with iQ SYBR Green Supermix (Bio-Rad Laboratories, Hercules, CA) on the Mastercycler Realplex (Eppendorf,

Table 2. Primers Used for Quantitative RT-PCR

		5'-3'
Lpar5	Forward	GCTCCAGTGCCCTGACTATC
	Reverse	GGGAAGTGACAGGGTGAAGA
Cxcr3	Forward	TGCTAGATGCCTCGGACTTT
	Reverse	CGCTGACTCAGTAGCACAGC
Cxcl9	Forward	AAAATTTTCATCACGCCCTTG
	Reverse	TCTCCAGCTTGGTGAGGTCT
Cxcl10	Forward	CCCACGTGTTGAGATCATTG
	Reverse	CACTGGGTAAAGGGGAGTGA
Cxcl11	Forward	AGTAACGGCTGCGACAAAGT
	Reverse	GCATGTTCCAAGACAGCAGA
Il-10	Forward	AGCCGGGAAGACAATAACTG
	Reverse	TCATTTCCGATAAGGCTTGG
Lgr5	Forward	CACCAGCTTACCCCATGACT
	Reverse	CTCCTGCTCTAAGGCCACCAC
Olfm4	Forward	GCCAGATCTTGGCTCTGAAG
	Reverse	GCCAGTTGAGCTGAATCACA
Somc2	Forward	ACACTCTGGACCGAGCAAGT
	Reverse	GCATTGCACTGGCTTGTAGA
Ascl2	Forward	GGTGACTCCTGGTGGACCTA
	Reverse	TCCGGAAGATGGAAGATGTC
β -actin	Forward	AGCCATGTACGTAGCCATCC
	Reverse	TCTCAGCTGTGGTGGTGAAG

RT-PCR, reverse-transcription polymerase chain reaction.

Hamburg, Germany). PCR primer sequences are listed in Table 2.

Cytokine Array

Lpar5^{ff};RosaCre^{ERT} enteroids on day 2 of culture were treated with 4OHT or vehicle. Thirty-six hours later, conditioned medium was collected and concentrated with Amicon Ultra-4 centrifugal filters. Cytokine expression in the concentrated conditioned medium was determined by using the Proteome Profiler Mouse Cytokine Array Kit (Cat no. ARY006; R&D Systems), a membrane-based sandwich immunoassay, following the manufacturer's instruction.

Immunohistochemistry

Intestinal segments were fixed with 10% formalin, embedded in paraffin, and processed into sections at the 5- μ m thickness. Paraffin-embedded sections were deparaffinized and rehydrated in a graded series of xylene and ethanol, followed by an antigen-unmasking procedure via a pressure cooker and sodium citrate buffer (10 mM sodium citrate, 0.05% Tween 20, pH 6.0). Immunohistochemical staining for CC3 with anti-CC3 antibody (PA5-114687, 1:200; Invitrogen, Waltham, MA) was performed as in previously described.⁸³

Immunofluorescence, EdU, and TUNEL Staining

After flushing with cold PBS, small intestinal tissues were incubated overnight in 30% sucrose in PBS for cryoprotection. Six-micron cryostat sections were prepared and stored at -80 °C until needed. The frozen sections were

fixed with ice-cold 100% ethanol and acetone at the ratio of 1:1 for 10 minutes at -20°C . After fixation, tissues and cells were permeabilized with 0.2% Triton X-100 for 10 minutes, blocked in PBS containing 5% goat serum for 1 hour at room temperature prior to incubation overnight with anti-OLFM4 antibody (D6Y5A, 1:500 dilution; Cell Signaling Technology, Boston, MA), anti-GFP antibody (GFP-1020, 1:500 dilution; Aves Labs, Davis, CA), or anti-CD4 antibody (MAB554, 1:500 dilution; R&D Systems) at 4°C . Sections were then stained with Alexa Fluor 488 conjugated Goat anti-rabbit antibody (A11034, 1:500; Invitrogen), Alexa Fluor 488 conjugated Donkey anti-chicken antibody (703-545-155, 1:500 dilution; Jackson ImmunoResearch, West Grove, PA), or Alexa Fluor 488 conjugated Goat anti-mouse antibody (A28175, 1:1000 dilution, Invitrogen) for 1 hour at room temperature. EdU-labeled cells were stained using the Click-iT EdU Cell Proliferation kit (Thermo Fisher Scientific). TUNEL staining was performed on intestinal tissues and enteroids using in situ cell death detection kit (MilliporeSigma, St. Louis, MO) according to the manufacturer's instruction. Images were taken using a Nikon A1R HD confocal microscope (Nikon Instruments, Melville, NY).

Statistical Analysis

Statistical analysis was performed by unpaired Student's *t* test or 1-way or 2-way analysis of variance, followed by Tukey post hoc analysis using GraphPad Prism software version 9 (La Jolla, CA). Results are presented as mean \pm SD. A value of $P < .05$ was considered significant.

References

- Barker N, van de Wetering M, Clevers H. The intestinal stem cell. *Genes Dev* 2008;22:1856–2864.
- McCarthy N, Kraiczy J, Shivdasani RA. Cellular and molecular architecture of the intestinal stem cell niche. *Nat Cell Biol* 2020;22:1033–2041.
- Biton M, Haber AL, Rogel N, Burgin G, Beyaz S, Schnell A, Ashenberg O, Su CW, Smillie C, Shekhar K, Chen Z, Wu C, Ordovas-Montanes J, Alvarez D, Herbst RH, Zhang M, Tirosh I, Dionne D, Nguyen LT, Xifaras ME, Shalek AK, von Andrian UH, Graham DB, Rozenblatt-Rosen O, Shi HN, Kuchroo V, Yilmaz OH, Regev A, Xavier RJ. T helper cell cytokines modulate intestinal stem cell renewal and differentiation. *Cell* 2018; 175:1307–2320 e1322.
- Luster AD, Ravetch JV. Biochemical characterization of a gamma interferon-inducible cytokine (IP-10). *J Exp Med* 1987;166:1084–2097.
- Giladi A, Wagner LK, Li H, Dorr D, Medaglia C, Paul F, Shemer A, Jung S, Yona S, Mack M, Leutz A, Amit I, Mildner A. Cxcl10(+) monocytes define a pathogenic subset in the central nervous system during autoimmune neuroinflammation. *Nat Immunol* 2020;21:525–534.
- Harris DP, Bandyopadhyay S, Maxwell TJ, Willard B, DiCorleto PE. Tumor necrosis factor (TNF)-alpha induction of CXCL10 in endothelial cells requires protein arginine methyltransferase 5 (PRMT5)-mediated nuclear factor (NF)-kappaB p65 methylation. *J Biol Chem* 2014; 289:15328–25339.
- Dwinell MB, Luger N, Eckmann L, Kagnoff MF. Regulated production of interferon-inducible T-cell chemoattractants by human intestinal epithelial cells. *Gastroenterology* 2001;120:49–59.
- Bondar C, Araya RE, Guzman L, Rua EC, Chopita N, Chirido FG. Role of CXCR3/CXCL10 axis in immune cell recruitment into the small intestine in celiac disease. *PLoS One* 2014;9:e89068.
- Piper KP, Horlock C, Curnow SJ, Arrazi J, Nicholls S, Mahendra P, Craddock C, Moss PA. CXCL10-CXCR3 interactions play an important role in the pathogenesis of acute graft-versus-host disease in the skin following allogeneic stem-cell transplantation. *Blood* 2007; 110:3827–3832.
- Ostvik AE, Granlund AV, Bugge M, Nilsen NJ, Torp SH, Waldum HL, Damås JK, Espevik T, Sandvik AK. Enhanced expression of CXCL10 in inflammatory bowel disease: potential role of mucosal Toll-like receptor 3 stimulation. *Inflamm Bowel Dis* 2013;19:265–274.
- Hyun JG, Lee G, Brown JB, Grimm GR, Tang Y, Mittal N, Dirisina R, Zhang Z, Fryer JP, Weinstock JV, Luster AD, Barrett TA. Anti-interferon-inducible chemokine, CXCL10, reduces colitis by impairing T helper-1 induction and recruitment in mice. *Inflamm Bowel Dis* 2005; 11:799–805.
- Sasaki S, Yoneyama H, Suzuki K, Suriki H, Aiba T, Watanabe S, Kawauchi Y, Kawachi H, Shimizu F, Matsushima K, Asakura H, Narumi S. Blockade of CXCL10 protects mice from acute colitis and enhances crypt cell survival. *Eur J Immunol* 2002;32:3197–3205.
- Omi J, Kano K, Aoki J. Current knowledge on the biology of lysophosphatidylserine as an emerging bioactive lipid. *Cell Biochem Biophys* 2021;79:497–508.
- Lee CW, Rivera R, Gardell S, Dubin AE, Chun J. GPR92 as a new G12/13- and Gq-coupled lysophosphatidic acid receptor that increases cAMP, LPA5. *J Biol Chem* 2006;281:23589–23597.
- Todorova MG, Fuentes E, Soria B, Nadal A, Quesada I. Lysophosphatidic acid induces Ca²⁺ mobilization and c-Myc expression in mouse embryonic stem cells via the phospholipase C pathway. *Cell Signal* 2009;21:523–528.
- Walker TL, Overall RW, Vogler S, Sykes AM, Ruhwald S, Lasse D, Ichwan M, Fabel K, Kempermann G. Lysophosphatidic acid receptor is a functional marker of adult hippocampal precursor cells. *Stem Cell Rep* 2016; 6:552–565.
- Valcarcel-Martin R, Martin-Suarez S, Muro-Garcia T, Pastor-Alonso O, Rodriguez de Fonseca F, Estivill-Torres G, Encinas JM. Lysophosphatidic acid receptor 1 specifically labels seizure-induced hippocampal reactive neural stem cells and regulates their division. *Front Neurosci* 2020;14:811.
- Hu HB, Song ZQ, Song GP, Li S, Tu HQ, Wu M, Zhang YC, Yuan JF, Li TT, Li PY, Xu YL, Shen XL, Han QY, Li AL, Zhou T, Chun J, Zhang XM, Li HY. LPA signaling acts as a cell-extrinsic mechanism to initiate cilia disassembly and promote neurogenesis. *Nat Commun* 2021;12:662.

19. Evseenko D, Latour B, Richardson W, Corselli M, Sahaghian A, Cardinal S, Zhu Y, Chan R, Dunn B, Crooks GM. Lysophosphatidic acid mediates myeloid differentiation within the human bone marrow microenvironment. *PLoS One* 2013;8:e63718.
20. Konno T, Kotani T, Setiawan J, Nishigaito Y, Sawada N, Imada S, Saito Y, Murata Y, Matozaki T. Role of lysophosphatidic acid in proliferation and differentiation of intestinal epithelial cells. *PLoS One* 2019;14:e0215255.
21. Choi S, Lee M, Shiu AL, Yo SJ, Aponte GW. Identification of a protein hydrolysate responsive G protein-coupled receptor in enterocytes. *Am J Physiol Gastrointest Liver Physiol* 2007;292:G98–G112.
22. Lin S, Yeruva S, He P, Singh AK, Zhang H, Chen M, Lamprecht G, de Jonge HR, Tse M, Donowitz M, Hogema BM, Chun J, Seidler U, Yun CC. Lysophosphatidic acid stimulates the intestinal brush border Na⁺/H⁺ exchanger 3 and fluid absorption via LPA5 and NHERF2. *Gastroenterology* 2010;138:649–658.
23. Jenkin KA, He P, Yun CC. Expression of lysophosphatidic acid receptor 5 is necessary for the regulation of intestinal Na⁽⁺⁾/H⁽⁺⁾ exchanger 3 by lysophosphatidic acid in vivo. *Am J Physiol Gastrointest Liver Physiol* 2018;315:G433–G442.
24. Wang M, He P, Han Y, Dong L, Yun CC. Control of intestinal epithelial permeability by lysophosphatidic acid receptor 5. *Cell Mol Gastroenterol Hepatol* 2021;12:1073–2092.
25. Choi S, Lee M, Shiu AL, Yo SJ, Hallden G, Aponte GW. GPR93 activation by protein hydrolysate induces CCK transcription and secretion in STC-1 cells. *Am J Physiol Gastrointest Liver Physiol* 2007;292:G1366–G1375.
26. Poole DP, Lee M, Tso P, Bunnett NW, Yo SJ, Lieu T, Shiu A, Wang JC, Nomura DK, Aponte GW. Feeding-dependent activation of enteric cells and sensory neurons by lymphatic fluid: evidence for a neurolymphocrine system. *Am J Physiol Gastrointest Liver Physiol* 2014;306:G686–G698.
27. Lin ME, Rivera RR, Chun J. Targeted deletion of LPA5 identifies novel roles for lysophosphatidic acid signaling in development of neuropathic pain. *J Biol Chem* 2012;287:17608–27617.
28. Bohin N, Carlson EA, Samuelson LC. Genome toxicity and impaired stem cell function after conditional activation of CreER(T2) in the intestine. *Stem Cell Rep* 2018;11:1337–2346.
29. Mathew D, Kremer KN, Strauch P, Tigyi G, Pelanda R, Torres RM. LPA5 is an inhibitory receptor that suppresses CD8 T-cell cytotoxic function via disruption of early TCR signaling. *Front Immunol* 2019;10:1159.
30. Lundquist A, Boyce JA. LPA5 is abundantly expressed by human mast cells and important for lysophosphatidic acid induced MIP-1 β release. *PLoS One* 2011;6:e18192.
31. Sato T, Vries RG, Snippert HJ, van de Wetering M, Barker N, Stange DE, van Es JH, Abo A, Kujala P, Peters PJ, Clevers H. Single Lgr5 stem cells build crypt-villus structures in vitro without a mesenchymal niche. *Nature* 2009;459:262–265.
32. Ireland H, Kemp R, Houghton C, Howard L, Clarke AR, Sansom OJ, Winton DJ. Inducible cre-mediated control of gene expression in the murine gastrointestinal tract: effect of loss of β -catenin. *Gastroenterology* 2004;126:1236–2246.
33. Schuijers J, van der Flier LG, van Es J, Clevers H. Robust cre-mediated recombination in small intestinal stem cells utilizing the *olm4* locus. *Stem Cell Rep* 2014;3:234–241.
34. Barker N, van Es JH, Kuipers J, Kujala P, van den Born M, Cozijnsen M, Haegebarth A, Korving J, Begthel H, Peters PJ, Clevers H. Identification of stem cells in small intestine and colon by marker gene *Lgr5*. *Nature* 2007;449:1003–2007.
35. Munoz J, Stange DE, Schepers AG, van de Wetering M, Koo BK, Itzkovitz S, Volckmann R, Kung KS, Koster J, Radulescu S, Myant K, Versteeg R, Sansom OJ, van Es JH, Barker N, van Oudenaarden A, Mohammed S, Heck AJ, Clevers H. The *Lgr5* intestinal stem cell signature: robust expression of proposed quiescent '+4' cell markers. *EMBO J* 2012;31:3079–3091.
36. Murata K, Jadhav U, Madha S, van Es J, Dean J, Cavazza A, Wucherpennig K, Michor F, Clevers H, Shivdasani RA. *Ascl2*-dependent cell dedifferentiation drives regeneration of ablated intestinal stem cells. *Cell Stem Cell* 2020;26:377–390.e6.
37. Goetzl EJ, Rosen H. Regulation of immunity by lysosphingolipids and their G protein-coupled receptors. *J Clin Invest* 2004;114:1531–2537.
38. Sui Y, Stehno-Bittel L, Li S, Loganathan R, Dhillon NK, Pinson D, Nath A, Kolson D, Narayan O, Buch S. CXCL10-induced cell death in neurons: role of calcium dysregulation. *Eur J Neurosci* 2006;23:957–964.
39. Sidahmed AM, Leon AJ, Bosinger SE, Banner D, Danesh A, Cameron MJ, Kelvin DJ. CXCL10 contributes to p38-mediated apoptosis in primary T lymphocytes in vitro. *Cytokine* 2012;59:433–441.
40. Sahin H, Borkham-Kamphorst E, do ONT, Berres ML, Kaldenbach M, Schmitz P, Weiskirchen R, Liedtke C, Streeck KL, Maedler K, Trautwein C, Wasmuth HE. Proapoptotic effects of the chemokine, CXCL 10 are mediated by the noncognate receptor TLR4 in hepatocytes. *Hepatology* 2013;57:797–805.
41. Otsuka H, Arimura N, Sonoda S, Nakamura M, Hashiguchi T, Maruyama I, Nakao S, Hafezi-Moghadam A, Sakamoto T. Stromal cell-derived factor-1 is essential for photoreceptor cell protection in retinal detachment. *Am J Pathol* 2010;177:2268–2277.
42. Woodruff TM, Arumugam TV, Shiels IA, Reid RC, Fairlie DP, Taylor SM. A potent human C5a receptor antagonist protects against disease pathology in a rat model of inflammatory bowel disease. *J Immunol* 2003;171:5514–5520.
43. Lammers KM, Lu R, Brownley J, Lu B, Gerard C, Thomas K, Rallabhandi P, Shea-Donohue T, Tamiz A, Alkan S, Netzel-Arnett S, Antalis T, Vogel SN, Fasano A. Gliadin induces an increase in intestinal permeability and zonulin release by binding to the chemokine receptor CXCR3. *Gastroenterology* 2008;135:194–204 e193.
44. Luster AD, Unkeless JC, Ravetch JV. Gamma-interferon transcriptionally regulates an early-response gene containing homology to platelet proteins. *Nature* 1985;315:672–676.

45. Castro F, Cardoso AP, Goncalves RM, Serre K, Oliveira MJ. Interferon-gamma at the crossroads of tumor immune surveillance or evasion. *Front Immunol* 2018;9:847.
46. Metzemaekers M, Vanheule V, Janssens R, Struyf S, Proost P. Overview of the mechanisms that may contribute to the non-redundant activities of interferon-inducible CXC chemokine receptor 3 ligands. *Front Immunol* 2017;8:1970.
47. Fu YY, Egorova A, Sobieski C, Kuttiyara J, Calafiore M, Takashima S, Clevers H, Hanash AM. T cell Recruitment to the Intestinal Stem Cell Compartment Drives immune-mediated intestinal damage after allogeneic transplantation. *Immunity* 2019;51:90–203.e3.
48. Bankaitis ED, Ha A, Kuo CJ, Magness ST. Reserve stem cells in intestinal homeostasis and injury. *Gastroenterology* 2018;155:1348–2361.
49. Powell AE, Wang Y, Li Y, Poulin EJ, Means AL, Washington MK, Higginbotham JN, Juchheim A, Prasad N, Levy SE, Guo Y, Shyr Y, Aronow BJ, Haigis KM, Franklin JL, Coffey RJ. The pan-ErbB negative regulator Lrig1 is an intestinal stem cell marker that functions as a tumor suppressor. *Cell* 2012;149:146–258.
50. Haber AL, Biton M, Rogel N, Herbst RH, Shekhar K, Smillie C, Burgin G, Delorey TM, Howitt MR, Katz Y, Tirosch I, Beyaz S, Dionne D, Zhang M, Raychowdhury R, Garrett WS, Rozenblatt-Rosen O, Shi HN, Yilmaz O, Xavier RJ, Regev A. A single-cell survey of the small intestinal epithelium. *Nature* 2017;551:333–339.
51. Tian H, Biehs B, Warming S, Leong KG, Rangell L, Klein OD, de Sauvage FJ. A reserve stem cell population in small intestine renders Lgr5-positive cells dispensable. *Nature* 2011;478:255–259.
52. Tan SH, Phuah P, Tan LT, Yada S, Goh J, Tomaz LB, Chua M, Wong E, Lee B, Barker N. A constant pool of Lgr5(+) intestinal stem cells is required for intestinal homeostasis. *Cell Rep* 2021;34:108633.
53. No YR, He P, Yoo BK, Yun CC. Regulation of NHE3 by lysophosphatidic acid is mediated by phosphorylation of NHE3 by RSK2. *Am J Physiol Cell Physiol* 2015;309:C14–C21.
54. Yoo BK, He P, Lee SJ, Yun CC. Lysophosphatidic acid 5 receptor induces activation of Na(+)/H(+) exchanger 3 via apical epidermal growth factor receptor in intestinal epithelial cells. *Am J Physiol Cell Physiol* 2011;301:C1008–C1016.
55. Mills GB, Moolenaar WH. The emerging role of lysophosphatidic acid in cancer. *Nat Rev Cancer* 2003;3:582–591.
56. Yu FX, Zhao B, Panupinthu N, Jewell JL, Lian I, Wang LH, Zhao J, Yuan H, Tumaneng K, Li H, Fu XD, Mills GB, Guan KL. Regulation of the Hippo-YAP pathway by G-protein-coupled receptor signaling. *Cell* 2012;150:780–791.
57. Yung YC, Stoddard NC, Chun J. LPA receptor signaling: pharmacology, physiology, and pathophysiology. *J Lipid Res* 2014;55:1192–2214.
58. Wang HC, Dann SM, Okhuysen PC, Lewis DE, Chappell CL, Adler DG, White AC Jr. High levels of CXCL10 are produced by intestinal epithelial cells in AIDS patients with active cryptosporidiosis but not after reconstitution of immunity. *Infect Immun* 2007;75:481–487.
59. Dufour JH, Dziejman M, Liu MT, Leung JH, Lane TE, Luster AD. IFN-gamma-inducible protein 10 (IP-10; CXCL10)-deficient mice reveal a role for IP-10 in effector T cell generation and trafficking. *J Immunol* 2002;168:3195–3204.
60. Peperzak V, Veraar EA, Xiao Y, Babala N, Thiadens K, Brugmans M, Borst J. CD8+ T cells produce the chemokine CXCL10 in response to CD27/CD70 costimulation to promote generation of the CD8+ effector T cell pool. *J Immunol* 2013;191:3025–3036.
61. Zumwalt TJ, Arnold M, Goel A, Boland CR. Active secretion of CXCL10 and CCL5 from colorectal cancer microenvironments associates with GranzymeB+ CD8+ T-cell infiltration. *Oncotarget* 2015;6:2981–2991.
62. Burke SJ, Goff MR, Lu D, Proud D, Karlstad MD, Collier JJ. Synergistic expression of the CXCL10 gene in response to IL-1beta and IFN-gamma involves NF-kappaB, phosphorylation of STAT1 at Tyr701, and acetylation of histones H3 and H4. *J Immunol* 2013;191:323–336.
63. Chen P, Vu T, Narayanan A, Sohn W, Wang J, Boedigheimer M, Welcher AA, Sullivan B, Martin DA, Ruixo JJ, Ma P. Pharmacokinetic and pharmacodynamic relationship of AMG 811, an anti-IFN-gamma IgG1 monoclonal antibody, in patients with systemic lupus erythematosus. *Pharm Res* 2015;32:640–653.
64. Walrath T, Malizia RA, Zhu X, Sharp SP, D'Souza SS, Lopez-Soler R, Parr B, Karchner B, Lee EC, Stain SC, Iwakura Y, O'Connor W Jr. IFN-gamma and IL-17A regulate intestinal crypt production of CXCL10 in the healthy and inflamed colon. *Am J Physiol Gastrointest Liver Physiol* 2020;318:G479–G489.
65. Tebo JM, Kim HS, Gao J, Armstrong DA, Hamilton TA. Interleukin-10 suppresses IP-10 gene transcription by inhibiting the production of class I interferon. *Blood* 1998;92:4742–4749.
66. Ciesielska A, Hromada-Judycka A, Ziemińska E, Kwiatkowska K. Lysophosphatidic acid up-regulates IL-10 production to inhibit TNF-alpha synthesis in Mvarphis stimulated with LPS. *J Leukoc Biol* 2019;106:1285–2301.
67. Plastira I, Joshi L, Bernhart E, Schoene J, Specker E, Nazare M, Sattler W. Small-molecule lysophosphatidic acid receptor 5 (LPA5) antagonists: versatile pharmacological tools to regulate inflammatory signaling in BV-2 microglia cells. *Front Cell Neurosci* 2019;13:531.
68. van Meeteren LA, Ruurs P, Stortelers C, Bouwman P, van Rooijen MA, Pradere JP, Pettit TR, Wakelam MJ, Saulnier-Blache JS, Mummery CL, Moolenaar WH, Jonkers J. Autotaxin, a secreted lysophospholipase D, is essential for blood vessel formation during development. *Mol Cell Biol* 2006;26:5015–5022.
69. Fotopoulou S, Oikonomou N, Grigorieva E, Nikitopoulou I, Paparountas T, Thanassopoulou A, Zhao Z, Xu Y, Kontoyiannis DL, Remboutsika E, Aidinis V. ATX expression and LPA signalling are vital for

- the development of the nervous system. *Dev Biol* 2010; 339:451–464.
70. Lin S, Haque A, Raeman R, Guo L, He P, Denning TL, El-Rayes B, Moolenaar WH, Yun CC. Autotaxin determines colitis severity in mice and is secreted by B cells in the colon. *FASEB J* 2019;33:3623–3635.
 71. El-Brolosy MA, Stainier D.Y.R. Genetic compensation: a phenomenon in search of mechanisms. *PLoS Genet* 2017;13:e1006780.
 72. Hozumi H, Hokari R, Kurihara C, Narimatsu K, Sato H, Sato S, Ueda T, Higashiyama M, Okada Y, Watanabe C, Komoto S, Tomita K, Kawaguchi A, Nagao S, Miura S. Involvement of autotaxin/lysophospholipase D expression in intestinal vessels in aggravation of intestinal damage through lymphocyte migration. *Lab Invest* 2013; 93:508–519.
 73. Kanda H, Newton R, Klein R, Morita Y, Gunn MD, Rosen SD. Autotaxin, an ectoenzyme that produces lysophosphatidic acid, promotes the entry of lymphocytes into secondary lymphoid organs. *Nat Immunol* 2008;9:415–423.
 74. Ellinghaus D, Folseraas T, Holm K, Ellinghaus E, Melum E, Balschun T, Laerdahl JK, Shiryaev A, Gotthardt DN, Weismuller TJ, Schramm C, Wittig M, Bergquist A, Bjornsson E, Marschall HU, Vatn M, Teufel A, Rust C, Gieger C, Wichmann HE, Runz H, Sterneck M, Rupp C, Braun F, Weersma RK, Wijmenga C, Ponsioen CY, Mathew CG, Rutgeerts P, Vermeire S, Schrupf E, Hov JR, Manns MP, Boberg KM, Schreiber S, Franke A, Karlsen TH. Genome-wide association analysis in primary sclerosing cholangitis and ulcerative colitis identifies risk loci at GPR35 and TCF4. *Hepatology* 2013;58:1074–2083.
 75. Imielinski M, Baldassano RN, Griffiths A, Russell RK, Annese V, Dubinsky M, Kugathasan S, Bradfield JP, Walters TD, Sleiman P, Kim CE, Muise A, Wang K, Glessner JT, Saeed S, Zhang H, Frackelton EC, Hou C, Flory JH, Otieno G, Chiavacci RM, Grundmeier R, Castro M, Latiano A, Dallapiccola B, Stempak J, Abrams DJ, Taylor K, McGovern D, Heyman MB, Ferry GD, Kirschner B, Lee J, Essers J, Grand R, Stephens M, Levine A, Piccoli D, Van Limbergen J, Cucchiara S, Monos DS, Guthery SL, Denson L, Wilson DC, Grant SFA, Daly M, Silverberg MS, Satsangi J, Hakonarson H. Common variants at five new loci associated with early-onset inflammatory bowel disease. *Nat Genet* 2009;41:1335–2340.
 76. Mackenzie AE, Lappin JE, Taylor DL, Nicklin SA, Milligan G. GPR35 as a novel therapeutic target. *Front Endocrinol (Lausanne)* 2011;2:68.
 77. Kaya B, Donas C, Wuggenig P, Diaz OE, Morales RA, Melhem H, Swiss IBDCI, Hernandez PP, Kaymak T, Das S, Hruz P, Franc Y, Geier F, Ayata CK, Villablanca EJ, Niess JH. Lysophosphatidic acid-mediated GPR35 signaling in CX3CR1(+) macrophages regulates intestinal homeostasis. *Cell Rep* 2020;32:107979.
 78. Richardson TG, Sanderson E, Palmer TM, Ala-Korpela M, Ference BA, Davey Smith G, Holmes MV. Evaluating the relationship between circulating lipoprotein lipids and apolipoproteins with risk of coronary heart disease: a multivariable Mendelian randomisation analysis. *PLoS Med* 2020;17:e1003062.
 79. Singh S, Singh H, Loftus EV Jr, Pardi DS. Risk of Cerebrovascular accidents and ischemic heart disease in patients with inflammatory bowel disease: a systematic review and meta-analysis. *Clin Gastroenterol Hepatol* 2014;12:382–393.e381.
 80. Kirchgessner J, Beaugerie L, Carrat F, Andersen NN, Jess T, Schwarzing M. Increased risk of acute arterial events in young patients and severely active IBD: a nationwide French cohort study. *Gut* 2018; 67:1261–2268.
 81. Baena-Díez JM, Garcia-Gil M, Comas-Cufí M, Ramos R, Prieto-Alhambra D, Salvador-González B, Elosua R, Dégano IR, Peñafiel J, Grau M. Association between chronic immune-mediated inflammatory diseases and cardiovascular risk. *Heart* 2018;104:119–226.
 82. Lim JF, Berger H, Su IH. Isolation and activation of murine lymphocytes. *J Vis Exp* 2016;116:54596.
 83. Lee SJ, Leoni G, Neumann PA, Chun J, Nusrat A, Yun CC. Distinct phospholipase C-beta isozymes mediate lysophosphatidic acid receptor 1 effects on intestinal epithelial homeostasis and wound closure. *Mol. Cell. Biol* 2013;33:2016–2028.

Received December 28, 2021. Accepted March 29, 2022.

Correspondence

Address correspondence to: Chris Yun, PhD, Division of Digestive Diseases, Emory University School of Medicine, Atlanta, GA 30324. e-mail: ccyun@emory.edu; fax: (404) 727-5767.

Acknowledgments

The authors thank Prof. Douglas J. Winton at the Cancer Research UK Cambridge Institute for providing AhCre mice.

CRedit Authorship Contribution

Zhongxing Liang (Conceptualization: Supporting; Data curation: Equal; Formal analysis: Equal; Methodology: Equal; Writing – review & editing: Supporting)

Peijian He (Conceptualization: Supporting; Data curation: Equal; Formal analysis: Equal; Methodology: Equal; Writing – original draft: Supporting)

Yiran Han (Data curation: Supporting; Formal analysis: Supporting; Methodology: Supporting)

Chris Yun, Ph.D. (Conceptualization: Lead; Funding acquisition: Lead; Supervision: Lead; Writing – original draft: Lead; Writing – review & editing: Lead)

Conflicts of Interest

The authors declare that there is nothing to disclose.

Funding

This work was supported by the grant from the National Institutes of Health (R01DK116799) and the Veterans Administration Merit Award (I01BX004459). Confocal microscopic analyses were supported in part by the Integrated Cellular Imaging Shared Resources of Winship Cancer Institute of Emory University and National Institutes of Health/National Cancer Institute under award P30CA138292.